

University of Pardubice

Faculty of Chemical Technology

Institute of Organic Chemistry and Technology



Functional High Performance Colorants

Ing. Fouzy Alafid

DISSERTATION THESIS

Supervisor: Prof. Ing. Radim Hrdina, CSc.

2023

The aim of the work

The main goal of this dissertation is the development of new organic colorants, especially pigments, which will have anti-corrosion properties in addition to their colour.

In order for an organic colorant to have anti-corrosion properties, it must also have antimicrobial properties.

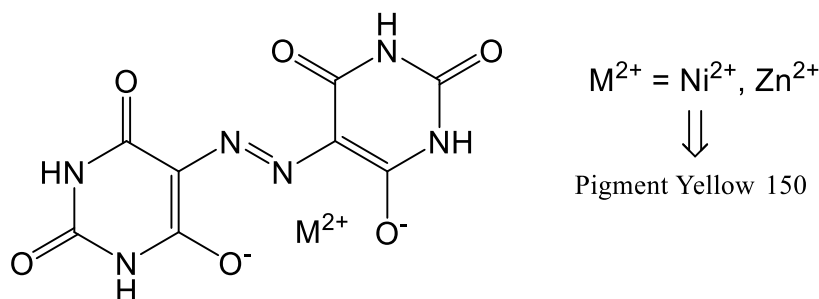
Literature background research pointed out the capability of using azobarbituric acid pigment (PY 150) and perylene pigments (PR 179, PR 149, PB 31) in functional organic colourants.

Summary

The main goal of this dissertation is the development of new organic colorants, especially pigments, which will have anti-corrosion properties in addition to their colour.

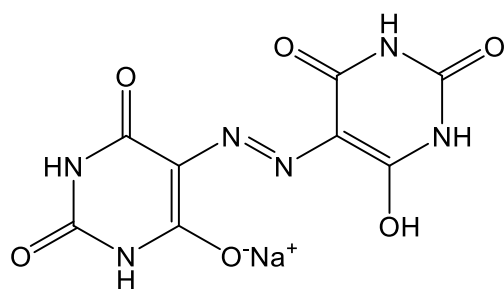
In order for an organic colorant to have anti-corrosion properties, it must also have antimicrobial properties.

The literary background research pointed out the capability of using azobarbituric acid pigment (PY 150) and perylene pigments (PR 179, PR 149, PB 31) in functional organic colorants. Thus, the series of pigments were prepared by reactions of azobarbituric acid with nickel chloride or zinc chloride and formed pigments were analyzed and tested.

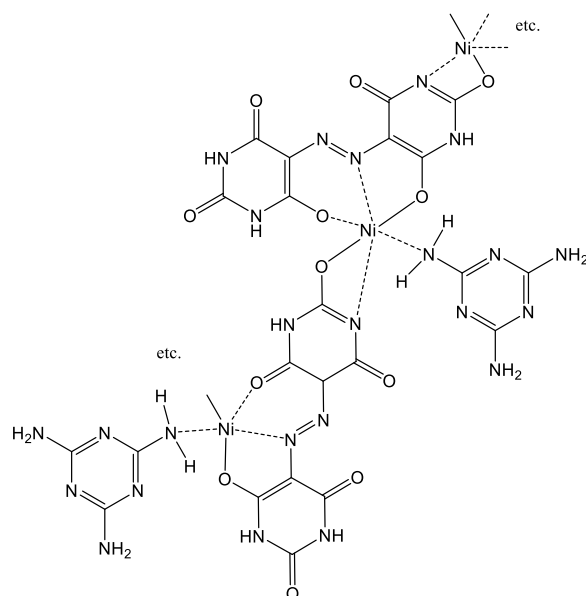


simplified chemical structure

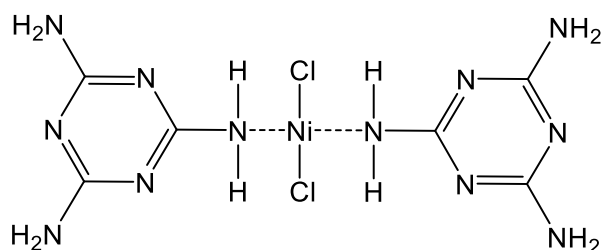
Special attention was paid to the commercial pigment Pigment Yellow 150 (PY 150), as the manufacturers of this pigment describe it as a complex of Ni^{2+} and azobarbituric acid. Furthermore, because the resulting pigment is very hard and difficult to disperse when used, they "intercalate melamine" into its crystal lattice. However, the logic of the matter says that if it was a mere intercalation, a softer pigment would not have been created. In studying the actual structure of PY 150, the structure of the starting azobarbituric acid, specifically the monosodium salt of azobarbituric acid, was first studied, which was determined to be:



Another study of this work showed that the monosodium salt of azobarbituric acid, melamine and nickel cation form a complex where Ni^{2+} has a coordination number of 6 and that this complex has a "polymeric character":

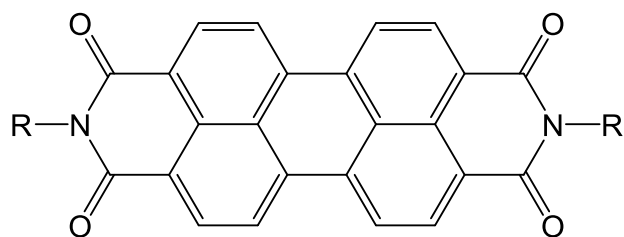


As part of this study, a new method for the production of PY 150 was developed, which is first based on the synthesis of the intermediate from melamine and nickel chloride:



followed by reaction with the monosodium salt of azobarbituric acid. This process is protected by the patent CZ 304515 B6 20140611 and the pigment produced by this procedure is in the portfolio of Synthesia a.s. under the name Versal Yellow 9GP.

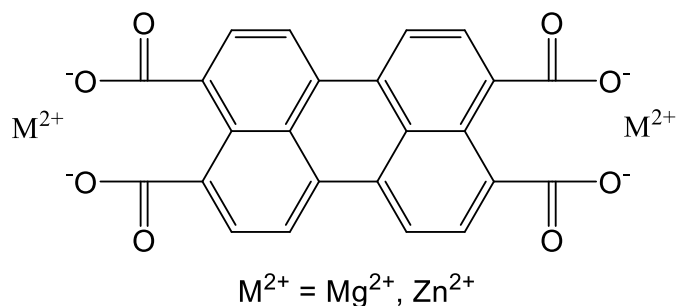
The perylene pigments were prepared by reactions of perylenetetracarboxylic dianhydride with methylamine or 3,5-dimethylaniline or 2-phenethylamine.



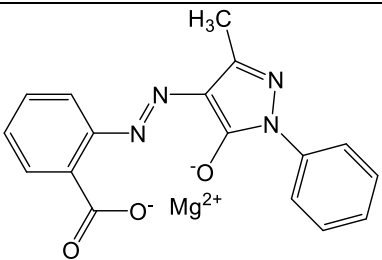
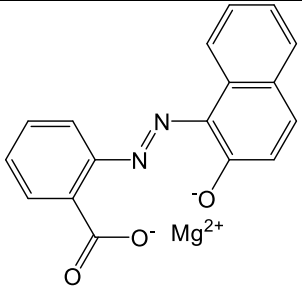
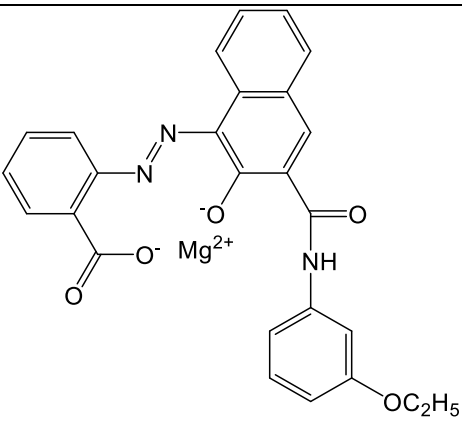
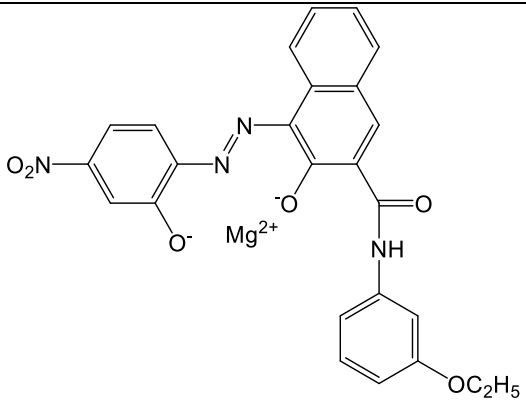
R	Commercial pigment
CH ₃ —	Pigment Red 179
	Pigment Red 149
	Pigment Black 31

Since it turned out that prepared pigments have no anti-corrosion or antimicrobial properties, additives with these properties were subsequently synthesised in this work.

Firstly, the series of anti-corrosion inhibitor compounds were prepared by reactions of perylenetetracarboxylic dianhydride with magnesium chloride or zinc chloride.

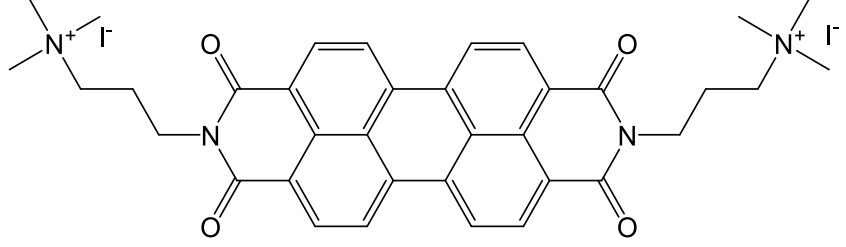
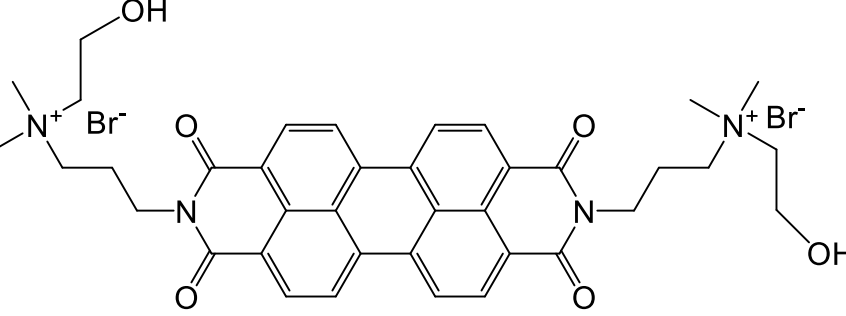
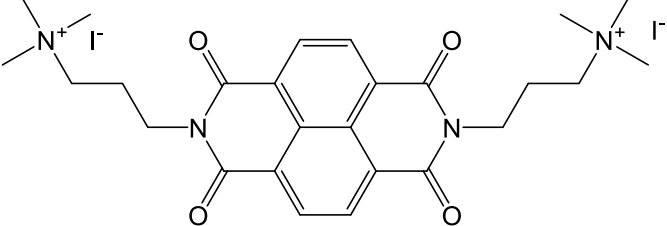
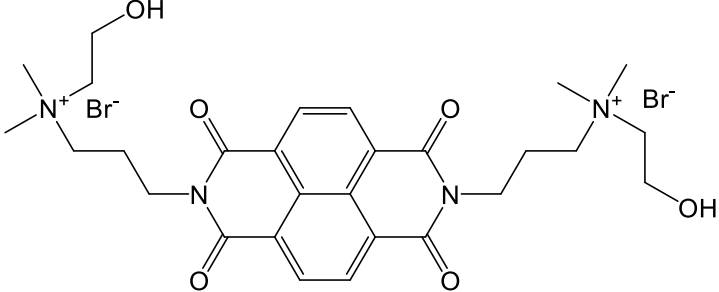


Also, the series of magnesium complexes with an azo carboxylate ligands (prepared by diazo-coupling reaction of anthranilic acid with 5-methyl-2-phenyl-3-pyrazolone, anthranilic acid with naphthol AS-PH, anthranilic acid with 2-naphthol and 2-amino-5-nitrophenol with naphthol AS-PH) were prepared.

Structure	Hue
 <p>The structure shows a perylene core with a phenyl group at position 1, a methyl group at position 2, and a carboxylate group at position 3. The carboxylate group is coordinated to a magnesium ion (Mg²⁺).</p>	Yellow
 <p>The structure shows a perylene core with a naphthalene group at position 1 and a carboxylate group at position 3. The carboxylate group is coordinated to a magnesium ion (Mg²⁺).</p>	Red
 <p>The structure shows a perylene core with a naphthalene group at position 1, a carboxylate group at position 3, and an ethyl ester group at position 4. The carboxylate group is coordinated to a magnesium ion (Mg²⁺).</p>	Red
 <p>The structure shows a perylene core with a nitro group at position 1, a carboxylate group at position 3, and an ethyl ester group at position 4. The carboxylate group is coordinated to a magnesium ion (Mg²⁺).</p>	Black

Because magnesium perylene-3,4,9,10-tetracarboxylate has shown excellent anti-corrosion properties, it is protected by the patent CZ 308991 (2020).

Secondly, the series of antimicrobial compounds were prepared in this work. From the chemical point of the view, these antimicrobial compounds are derivatives of perylene diimide prepared by the reaction of perylenetetracarboxylic dianhydride or naphthalene tetracarboxylic dianhydride with *N,N*-dimethyl-1,3-propanediamine. Consequently, alkylation with iodomethane or with 2-bromoethanol.

Structure	Hue
	Red
	Red
	Colorless
	Colorless

Finally, the relationship between their structure and anti-microbial effect was studied.

Keywords: organic pigment, metal complex, coating; corrosion; anti-corrosion efficiency, anti-microbial activity.

Chapter 1

1. Pigment based on azobarbituric acid

Introduction

Azo dyes and pigments are well known because of their use as colorants in the industry. Thousands of azo pigments of different structure variations have been prepared [1]. The metal salt for the making reaction between azobarbituric acid (Figure 1) (derivative) and metal salt is preferably selected from water-soluble metal salt, especially chlorides, bromides, acetates, or nitrates of the metal [2]. Pigment Yellow 150 (PY 150) is a yellow pigment based on azobarbituric acid as a ligand and the metal cation Ni^{2+} . The Colour Index (published by The Society of Dyers and Colourists and the American Association of Textile Chemists and Colorists) describes this pigment without specifying the structure and the type of binding of nickel to the azobarbituric acid. Thus, PY 150 is described as "a complex of nickel and azobarbituric acid" (Nickel, 5,5'-azobis-2,4,6(1H,3H,5H)-pyrimidinetrione complexe). Therefore, the chemical structure of the pigment is uniquely determined, its molecular weight as a chemical individual, not its crystal structure. In the professional literature it is assumed that this is a complex having a ligand-nickel ratio of (azobarbituric acid) 1:1 and having the following structure (Figure 2) [3]:

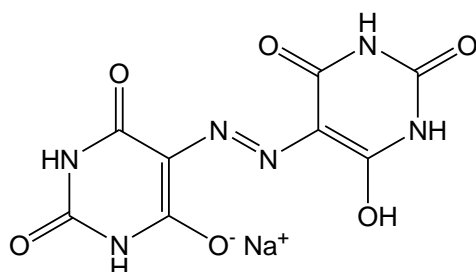


Figure 1. Structure of monosodium salt of azobarbituric acid.

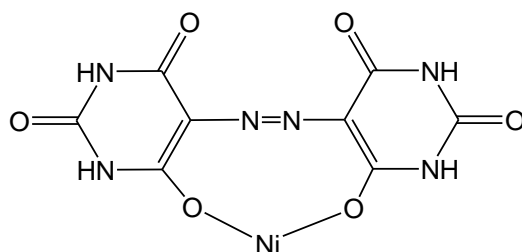


Figure 2. Complex nickel azobarbituric acid.

Although thus delineated structure indicates rather salt. It is assumed that a ligand can exist in many possible tautomeric forms, which have the same molecular formula $\text{C}_8\text{H}_4\text{N}_6\text{O}_6$.

azobarbituric acid (in the form of “free acid”) is a poly-dentate ligand, which theoretically can release 6 protons and form following electrostatic and covalent (coordination) (Figure 3).

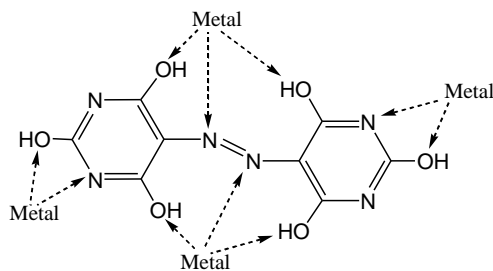


Figure 3. Structure of azobarbituric acid.

Melamine is a compound that can accept a proton to create groups that can form hydrogen bonds and electrostatic binding. Melamine has a dissociation constant in water at 25 °C $pK_a = 5$. Nickel ion Ni^{2+} itself can bind two anions and possible coordination numbers are 4, 5, 6. However, nickel is usually present in only one oxidation state (Ni^{2+}). Schematic cast d-orbitals in octahedral complexes (coordination number 6) show that these complexes should have two unpaired electrons and magnetic moments should vary from 2.9 to 3.4 BM. Bipyramidal trigonal complexes (coordination number 5) are often formed with polydentate ligands and are diamagnetic. A regular tetrahedral complex (coordination number 4) with four identical ligands should have a magnetic moment between 3.5 to 4.2 BM. Planar complex (coordination number 4) can be either diamagnetic or may have two unpaired electrons, depending on whether the energy difference of the two highest d-orbitals is larger or smaller than the energy required to pair electrons. The energy difference of the highest d-orbitals is specified by the nature and extent of the four ligands. Neighboring molecules contribute to the ligand field along the axis perpendicular to the square of the four ligand atoms. Experimental data show that only in the presence of two other molecules, which are quite good donors (and this may be the case with complex azobarbituric acid), the energy difference becomes so small that there is a paramagnetic complex. Indeed, purely square complexes (with coordination number 4), have a low spin and are diamagnetic.

Melamine (M) with Ni^{2+} , strictly speaking, with $NiCl_2 \cdot 6H_2O$, creates green octahedral complexes $[NiM_2Cl_2] \cdot 3H_2O$ or $[NiM_2Cl_2]$ [4]. (Figure 4.) [5].

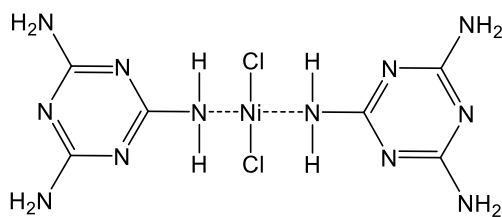


Figure 4. Nickle melamine intermediate.

Because PY 150 based on complex azobarbituric acid and nickel has poor properties, especially hardness and grain, already been proposed to intercalate into the crystal lattice acid complex with nickel azobarbituric another compound [6]. A possible inclusion compound is in the document mentioned melamine, which is eventually used in practice [7a,7b]. Later, then only specify dispersing hardness and pH of the water extract of these pigments. In the crystal lattice is intercalated another compound (melamine). A process of preparing a complex of nickel and azobarbituric acid intercalate melamine, where modifying the starting material to a mixture of mono- and di-cationic salts of cationic azobarbituric acid ultimately achieve constant pigment having specific surface area and narrow particle size distribution (in the document, however, particle size not measured) [8].

1.1. Reaction of azobarbituric acid with nickel and melamine

Background

Japanese document describes a process wherein the nickel complex is first prepared and the azobarbituric acid as a host compound, which intercalates melamine. This will provide the pigment that has a specific crystalline form having the powder X-ray diffraction spectrum (CuK α ray). The following peaks at Bragg angles ($2\theta, \pm 0.2^\circ$), 14.0° , 14.5° , 26.5° , 28° , 0° and 29.0° . This crystal structure of clathrates Pigment Yellow 150 is denoted as α . The same document describes the previous commercially available pigments of this type (CI Pigment Yellow 150 prepared by Bayer FANCHON Fast Yellow Y-5688), where these have the crystalline form, which has a powder X-ray diffraction spectrum (CuK α X-ray) of the following peaks at Bragg angles ($2\theta, \pm 0.2^\circ$), 8.9° , 18.5° , 20.2° , 23.6° , 26.3° and 27.5° . Denote the crystal structure of clathrates Pigment Yellow 150 as β [9].

In the market, Pigment Yellow 150 is a specific crystal structure called Bayplast Yellow 5GN. In powder X-ray diffraction pattern (CuK α) characterized by main peaks at Bragg angles ($2\theta, \pm 0.2^\circ$) 8.52° and 9.23° . The crystal form of the pigment is denoted as γ .

1.1.2. Results

1.1.3. Synthesis of melamine nickel intermediate

The reactions of melamine and nickel (intermediate) were carried out in butanol under mild condensation at pH 2, according to the general scheme shown in (Figure 5). The product of this reaction was isolated with high yields and sufficient purity. The theoretical content of Ni²⁺ was 15.37 %, found Ni²⁺ content in the intermediate was 13.3 %.

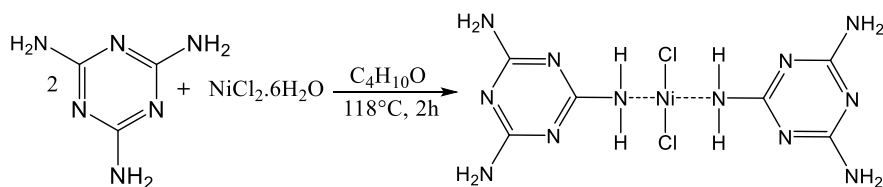


Figure 5. Nickel melamine intermediate.

1.1.4. Synthesis of Pigment Yellow 150: crystallized as ϵ modification

The reaction of the intermediate with azobarbituric acid in Pressure less reactor (PLR) was carried out in water under mild condensation for 14 hours at pH 5, according to the general scheme shown in (Figure 6). The product of this reaction was isolated with high yields and sufficient purity. The theoretical content of Ni^{2+} was 9.93 %, found Ni^{2+} content in the intermediate was 9.66 %.

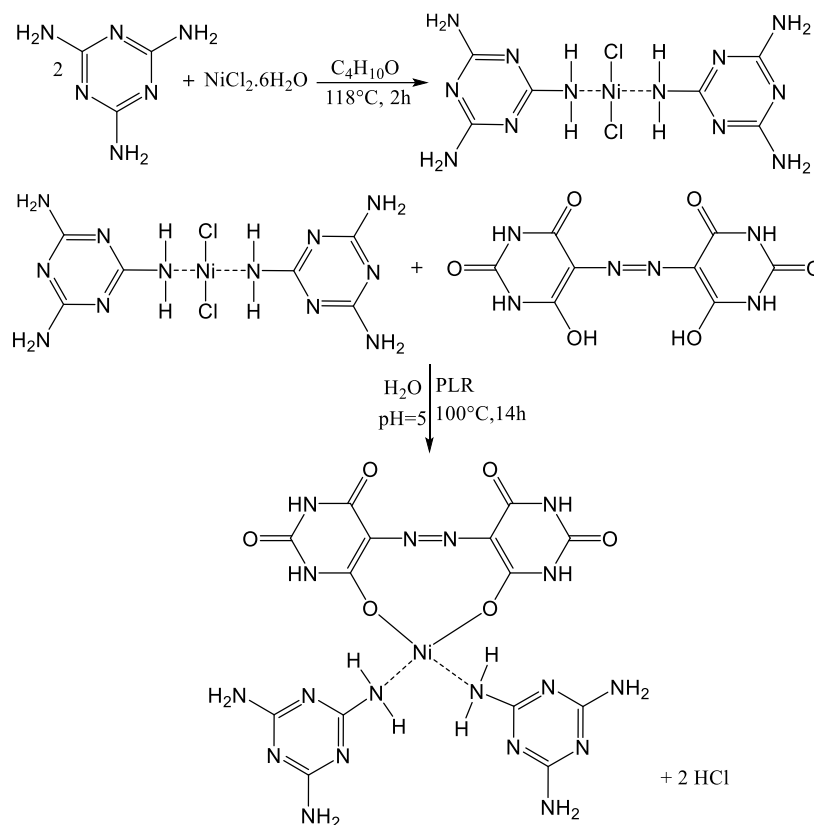


Figure 6. Synthesis of Pigment Yellow 150: crystallized as ϵ modification.

1.1.5. Synthesis of Pigment Yellow 150: crystallized as δ modification

The reaction of the intermediate with azobarbituric acid was carried out in water under pressure in an autoclave for 5 minutes at pH 2.1, according to the general scheme shown in (Figure 7). The product of this reaction was isolated with high yields and sufficient purity.

The theoretical content of Ni^{2+} was 9.93 %, found Ni^{2+} content in the intermediate was 8.99 %.

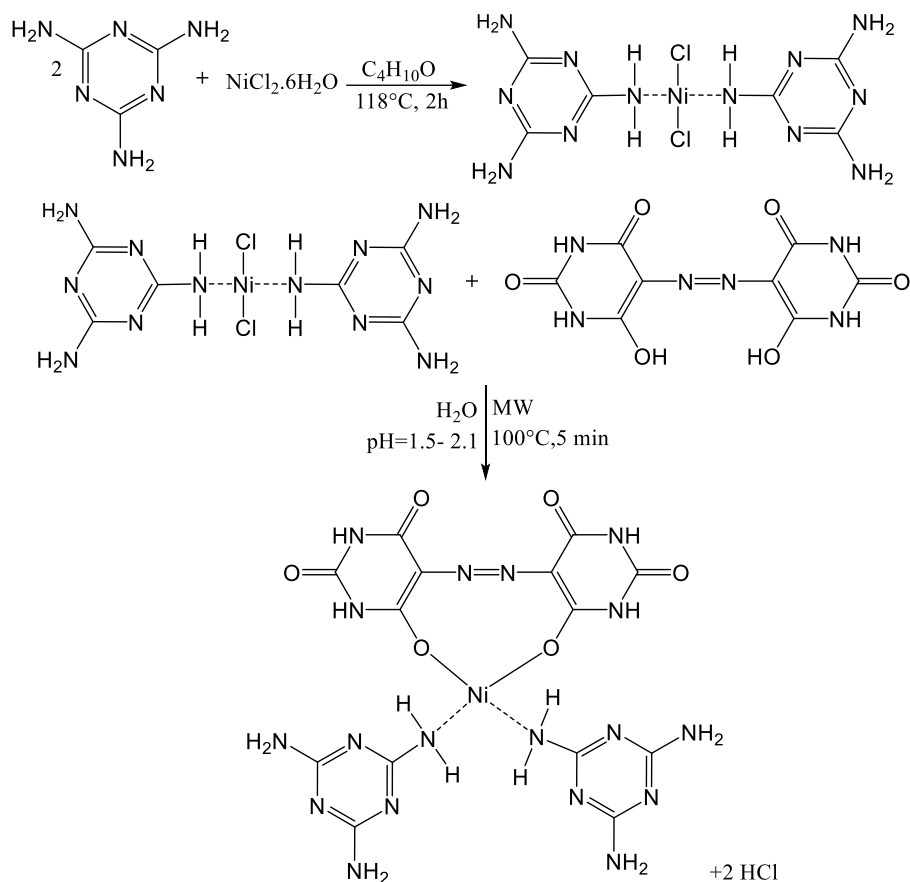


Figure 7. Synthesis of Pigment Yellow 150: crystallized as δ modification.

1.1.6. Synthesis of Zn-pigment and Cu-pigment

Synthesis melamine copper and melamine zinc intermediates in pressure less reactor (PLR). The reactions of melamine and copper or melamine and zinc (intermediate) were carried out in butanol under mild condensation, according to the general scheme shown in (Figure 8). The product of this reaction was isolated with high yields and sufficient purity. The theoretical content of Zn^{2+} was 16.83 %, found Zn^{2+} content in the intermediate was 14.79 %. And the theoretical content of Cu^{2+} was 16.43%, found Cu^{2+} content in the intermediate was 15.30 %.

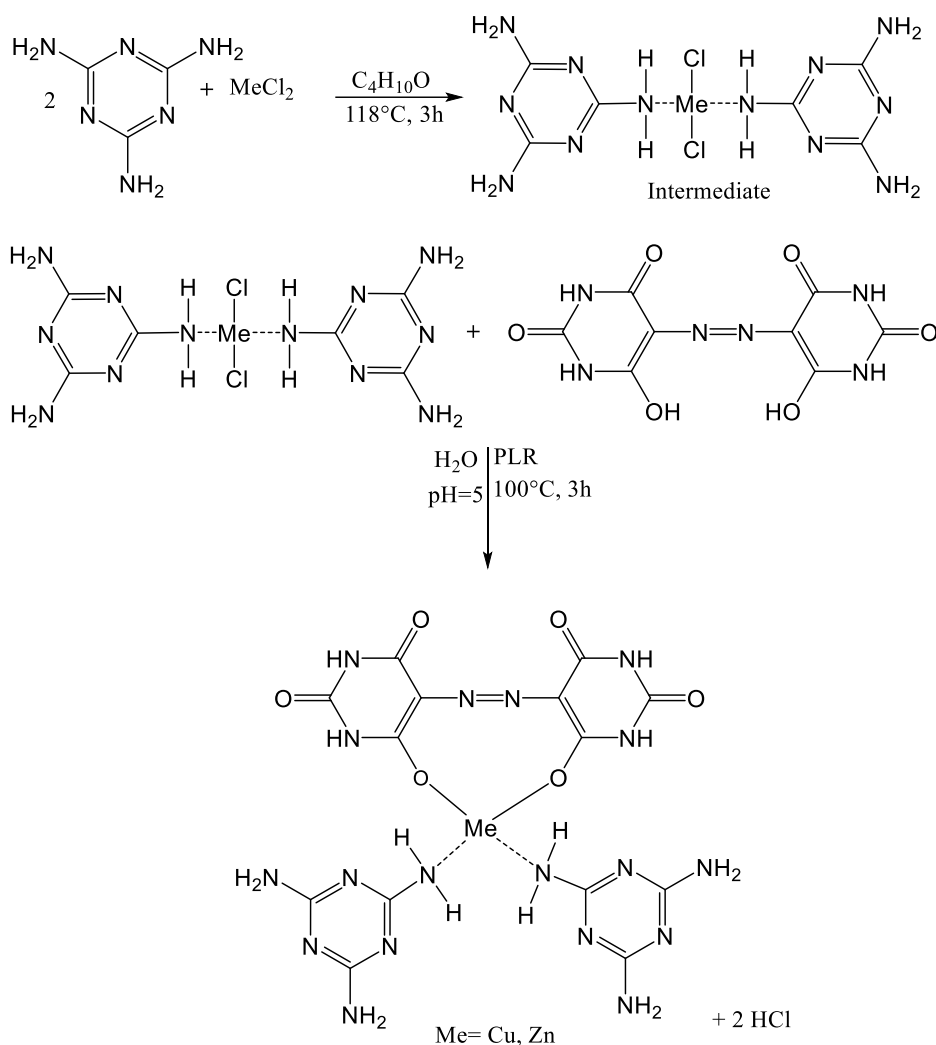


Figure 8. Synthesis of Cu-pigment and Zn-pigment.

1.1.7. Synthesis of Zn-pigment and Cu-pigment

The reactions of intermediate (Zu-intermediate or Cu-intermediate) with azobarbituric acid were carried out in water under mild conditions for 3 hours at pH 5, according to the general scheme shown in Figure 8. The product of this reaction was isolated with high yields and sufficient purity. The theoretical content of Zn^{2+} was 10.32 %, found Zn^{2+} content in the pigment was 10.73 %. And the theoretical content of Cu^{2+} was 10.06%, found Cu^{2+} content in the intermediate was 10.63 %.

1.2. NMR azobarbituric acid monosodium salt:

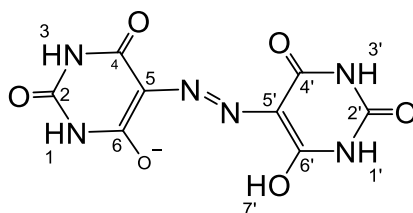


Figure 9. Azobarbituric acid monosodium salt

Table 1. ^1H and ^{13}C chemical shifts and the shape signal (DMSO- d_6 , 25 ° C) for azobarbituric acid monosodium salt.

H/C	$\delta(^1\text{H})$ [ppm]	$\delta(^{13}\text{C})$ [ppm]
1	10.45 (br s)	-
2	-	150.21
3	10.91 (br s)	-
4	-	158.86
5	-	109.78
6	-	162.71
1'	10.45 (br s)	-
2'	-	149.90
3'	10.91 (br s)	-
4'	-	158.86
5'	-	99.08
6'	-	161.96
7'	15.62 (s)	-

According to the NMR measurements, the sample is mono azobarbituric acid salt. In the ^1H NMR signals are only twice NH plus a typical signal for a single OH (enol). APT ^{13}C NMR spectrum also indicates only the presence of tert carbons, no CH group is not present. Therefore, arises anion deprotonation OH group. Instability was not a dimer in DMSO and 25 °C was observed (after a day of standing). Based on our own research, we concluded that the yellow pigment-based nickel complex cation, anion and melamine azobarbituric acid, prepared in this way, the formula $[\text{NiLMm}]_n$, where L is the anion azobarbituric acid ($\text{L} = \text{C}_8\text{H}_4\text{N}_6\text{O}_6$), M denotes melamine ($\text{C}_3\text{H}_6\text{N}_6$), $m = 0, 1$ or 2 , $n \geq 2$, and may contain water of crystallization.

^1H NMR spectrum is shown below. The strongest signals in the ^1H NMR spectrum belong incompletely deuterated solvent ($\delta = 2.55$) and residual water in the solvent ($\delta = 3.38$). The compound has six protons. After the substitution of one hydrogen in sodium left five protons that give the ^1H NMR spectrum of the corresponding signals.

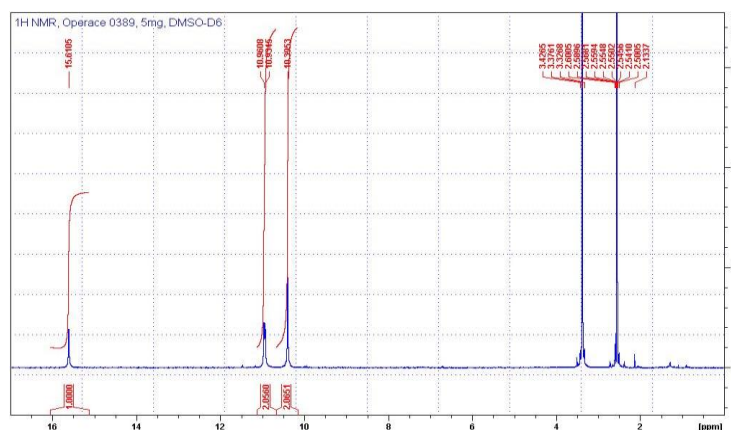


Figure 10. ^1H NMR spectrum in hexadeuteriodimethylsulfoxid.

1.2.1. NMR Melamine.

The ^{13}C CP/MAS NMR signals resonating at 168 ppm can be attributed to $-\text{HN}-\underline{\text{C}}(\text{NH}_2)=\text{N}-$ carbon atoms in the melamine molecule (Figure 11). The system seems to be highly ordered and crystalline as indicated by the narrow signals.

The observed asymmetric splitting of the signal in the ratio of 1:2 indicates that the carbon atoms are magnetically nonequivalent, probably due to the nonsymmetrical molecular packing in the crystal unit.

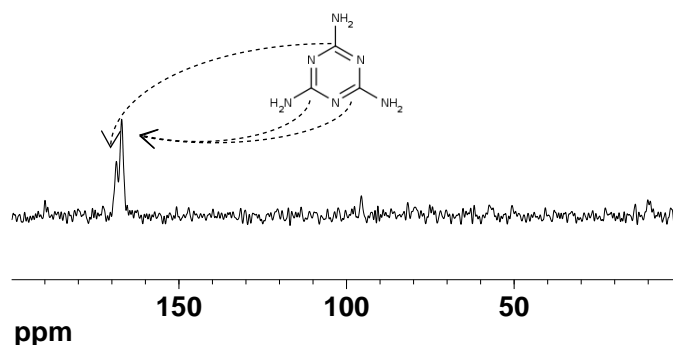


Figure 11. ^{13}C CP/MAS NMR spectrum of melamine and the proposed signal assignment.

1.2.2. NMR Melamine nickel intermediate:

The ^{13}C CP/MAS NMR spectrum of this system is dominated by two intensive signals resonating at ca. 165 and 152 ppm. Both these signals can be attributed to $-\text{HN}-\underline{\text{C}}(\text{NH}_2)=\text{N}-$ carbon atoms in the melamine molecule in the prepared complex (Figure 12). As indicated by the narrowing of these signals, the prepared is highly ordered (crystalline).

The observed low-intensive signals resonating at ca. 168 ppm probably correspond to the residual fraction of unconverted melamine. The amount of this fraction is less than 8%.

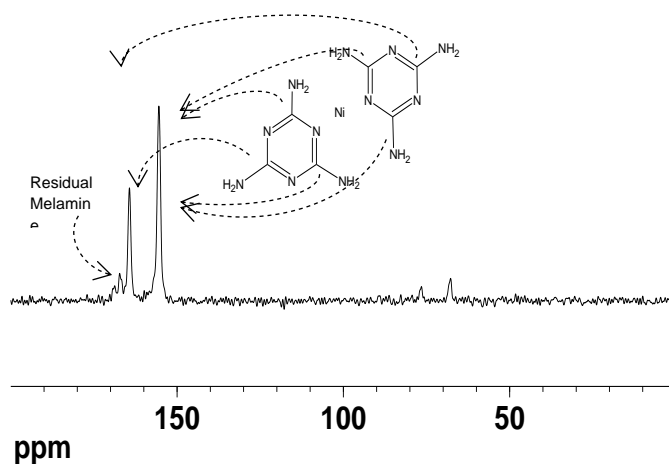


Figure 12. ^{13}C CP/MAS NMR spectrum of nickel melamine intermediate and the proposed signal assignment.

1.2.3. Bohr magneton:

The expected composition $[\text{NiCl}_2(\text{melamine})_2]$ supplied the most transparent results. Good bulk properties. Slight ferromagnetic interaction expressed value $\Theta = -28 \text{ K}$, the Curie-Weiss law (linear dependence of the reciprocal value of the corrected molar magnetic susceptibility on temperature) implies a magnetic moment $\mu = 2.92 \text{ B.M}$ in good agreement with the present two unpaired electrons.

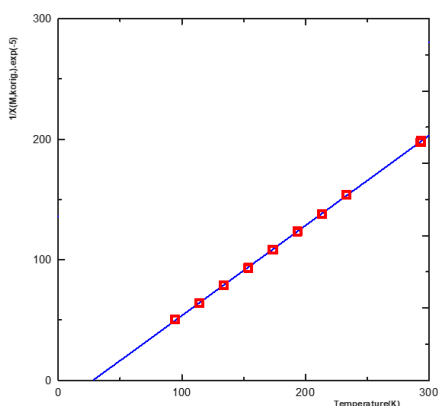


Figure 13. Melamine nickle intermediate.

1.2.4. Powder X-ray diffraction:

The pigment synthesis in the next synthetic step used azobarbituric acid monosodium salt (Synthesia a.s Pardubice), whose X-ray powder diffraction pattern - $\text{CuK}\alpha$ radiation - is shown in (Figures 14 and 15).

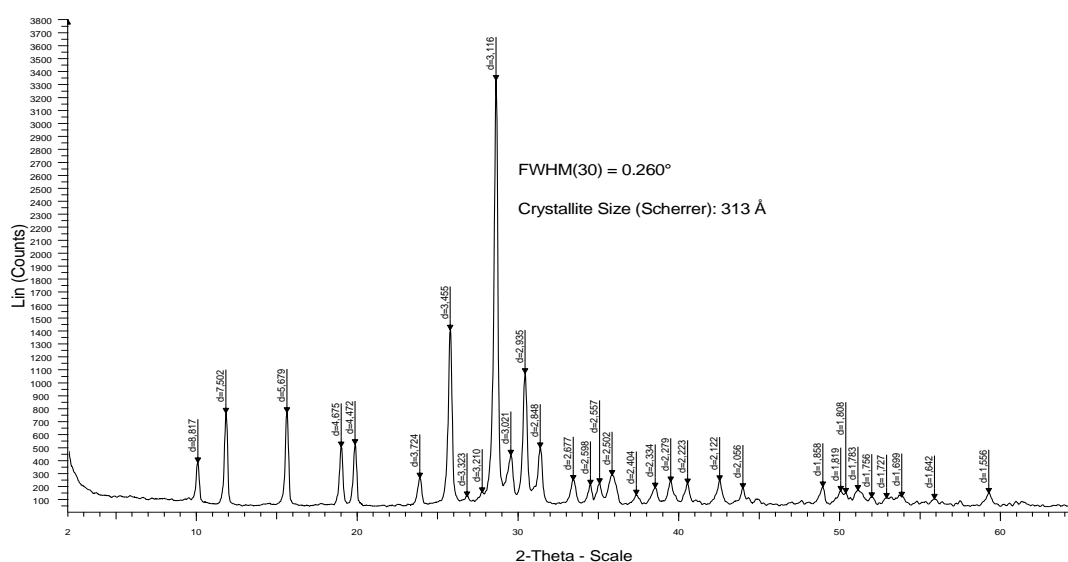


Figure 14. X-ray diffraction pattern azobarbituric acid monosodium salt before treatment.

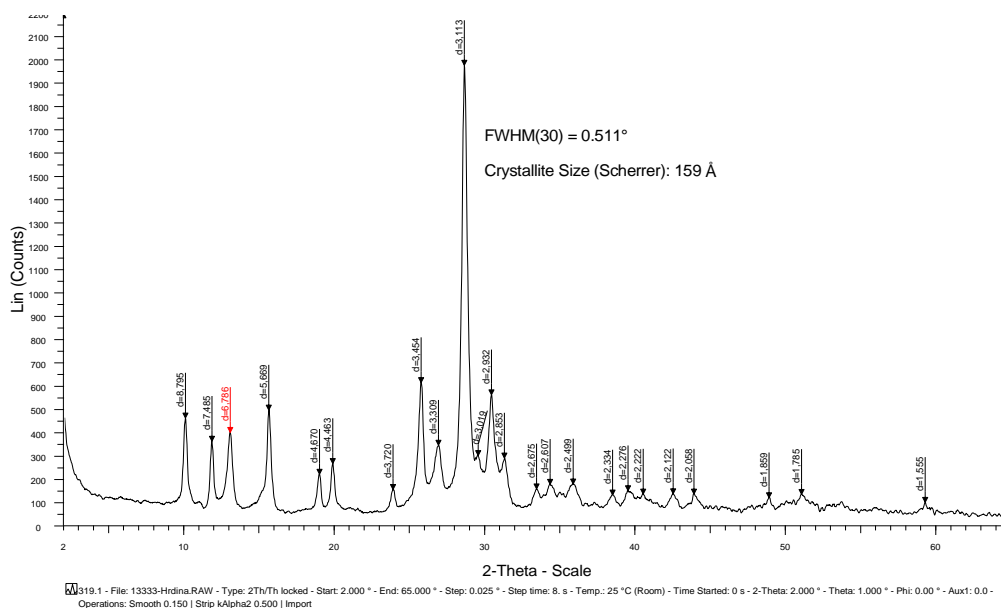


Figure 15. X-ray diffraction pattern azobarbituric acid monosodium salt after treatment.

The complex of nickel chloride and melamine, which is melamine nickel intermediate. The structure $\text{NiCl}_2(\text{C}_3\text{H}_6\text{N}_6)_2$ that intermediate may contain water of crystallization and a polymeric octahedral structure. With the following peaks, the yellow line is the diffraction pattern of pure melamine, the black line is the melamine nickel intermediate. The results indicate that the melamine nickel intermediate does not contain free melamine (Figure 16).

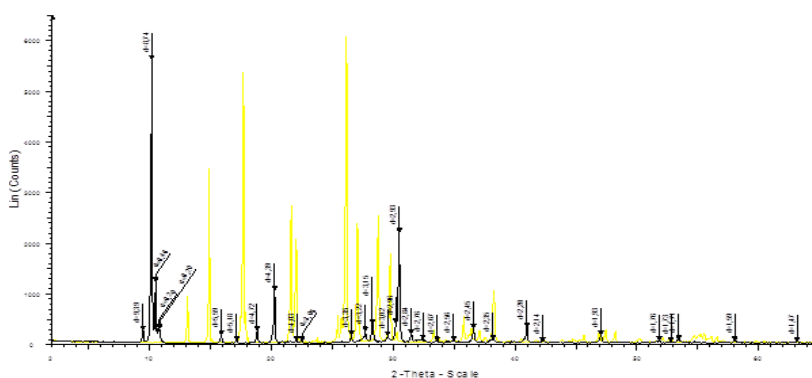


Figure 16. X-ray diffraction pattern of melamine and melamine nickel intermediate.

Pigment Yellow 150 crystal form ϵ has in powder X-ray diffraction pattern ($\text{CuK}\alpha$) of the following peaks at Bragg angles ($2\Theta, \pm 0.2^\circ$) and the next interplane distanced (Figure 17 and Table 2).

Table 3. X-ray diffraction pattern of crystal form pigment δ .

2θ	d [Å]	Relative intensity
7,39	11,98	14
9,68	9,17	67
9,94	8,89	45
14,06	6,34	13
14,82	5,97	43
19,99	4,43	28
20,34	4,38	13
27,37	3,27	30
27,92	3,19	100

1.2.5. Negative ESI mass spectrum of ABK.

ESI MS spectrum: In water solution, the base intensity ion was observed with nominal molecular weight 281 Daltons (deprotonated molecule ion $[M-H]^-$). Adduct ion $[2M-2H+Na]^-$ was also detected at $m/z=585$ with lower intensity.

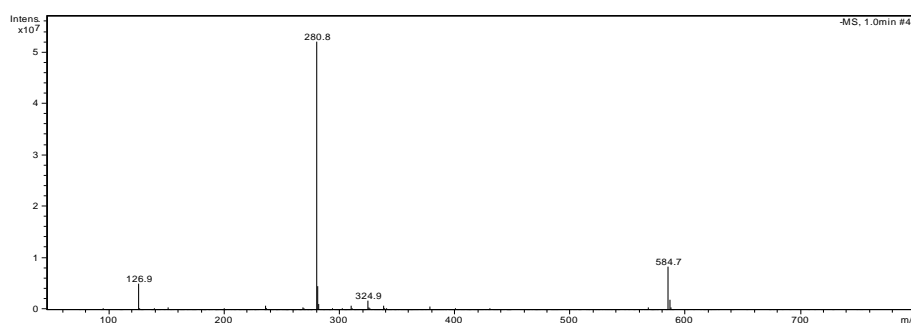
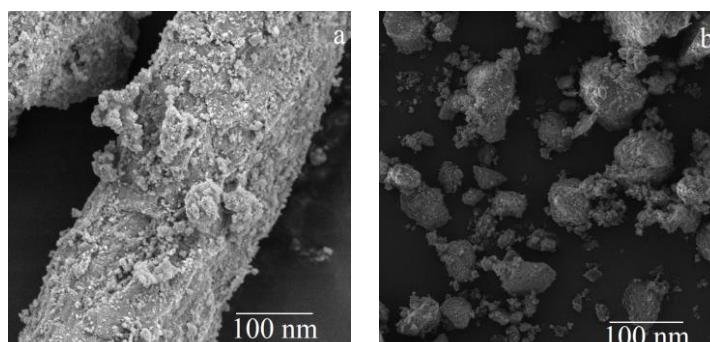


Figure 19. Negative ESI mass spectrum of water solution of azobarbituric acid.

1.2.6. EMS:

(a) Pigment Yellow 150 without melamine (b) is the compound from Lanxess Deutschland GmbH; (c) is the prepared compound with Crystal form ϵ ; (d) is the prepared compound with Crystal form δ , from the EMS images we can see that is no regular large crystals, but small crystals held together in a more or less spherical bodies with crystal size around 100 nm.



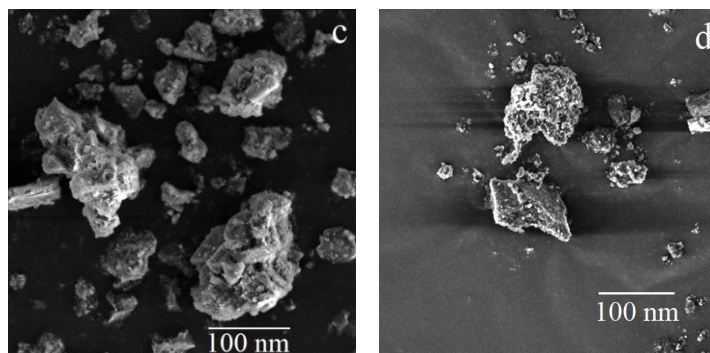


Figure 20. EMS images of lanxess compound and the prepared compounds.

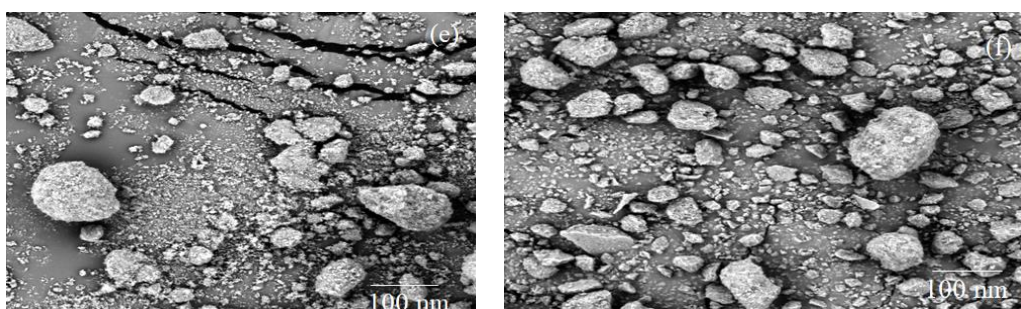


Figure 21. EMS images of (e) Zn-pigment and (f) Cu-pigment.

1.3. Conclusion:

From the X-ray powder results can be concluded, that after the acid treatment (HCl) of monosodium salt of azobarbituric acid still is monosodium salt, the size of the particles decreased (31.3 nm \rightarrow 15.9 nm) in the X-diffractogram appears one new peak (red line $d = 6.786$) (Figure 13), probably due to the reaction of basic $-NH-$ centrum with HCl. Azobarbituric acid mono salt sodium was confirmed by ESI MS spectrum in hydrazo form with the M.W. 282. The 1H NMR spectrum of the compound, there are four types of signals hydrocarbons ($\delta = 15.61$ (1H), 10.96 (1H), 10.93 (1H) and 10.40 (2H)), one of which has double the intensity. Therefore, the substance contains five atoms of hydrogen. This observation demonstrates a loss of a hydrogen atom in the compound molecule, and thus indirectly supports the presence of one sodium atom. The prepared Pigment Yellow 150 (PY 150) is a very lightfast and weather-fast yellow pigment with good heat stability. Main use of Pigment Yellow 150 is in the printing color and the formulation of paints. The yellow pigment has excellent application properties, which are comparable with the commercially produced pigments.

Chapter 2

2. Perylene pigments

Introduction

The name of perylene pigment is a class of high performance pigments made from *N,N'*-disubstituted perylene-3,4,9,10-tetracarboxylic acid imides or perylene-3,4,9,10-tetracarboxylic acid dianhydrides. The chemistry of perylene derivatives are well-known organic pigments on the market and have attracted attention as materials useful for electro photographic photoreceptors, photovoltaic elements, optical disks as well. Perylene pigments cover a variety of shades in the solid-state from vivid red (PR 149), via maroon (PR 179) to black (PB 31) [10]. Among the molecules of interest for applications in organic semiconductor devices, 3,4,9,10,-perylene-tetracarboxylic dianhydride (PTCDA) is one of the best investigated perylene derivatives. Experimental, vibrational modes in PTCDA powder, crystals and thin films were measured using Infrared or high-resolution electron energy loss spectroscopy [11].

2.1. Results

2.1.1. Synthesis of perylene pigments

The reactions were done under atmosphere pressure in an autoclave for PR 149, PB 31, and in conventional heating for PR 179. Solvents were removed by filtration using Buchner filtration. The reactions of PR 149 and PB 31 were carried out in the water in the autoclave for 23 hours, where the reaction of PR 179 was carried on under mild conditions for 8 hours, according to the general scheme shown in Figure 22. The product of this reaction was isolated with high yields.

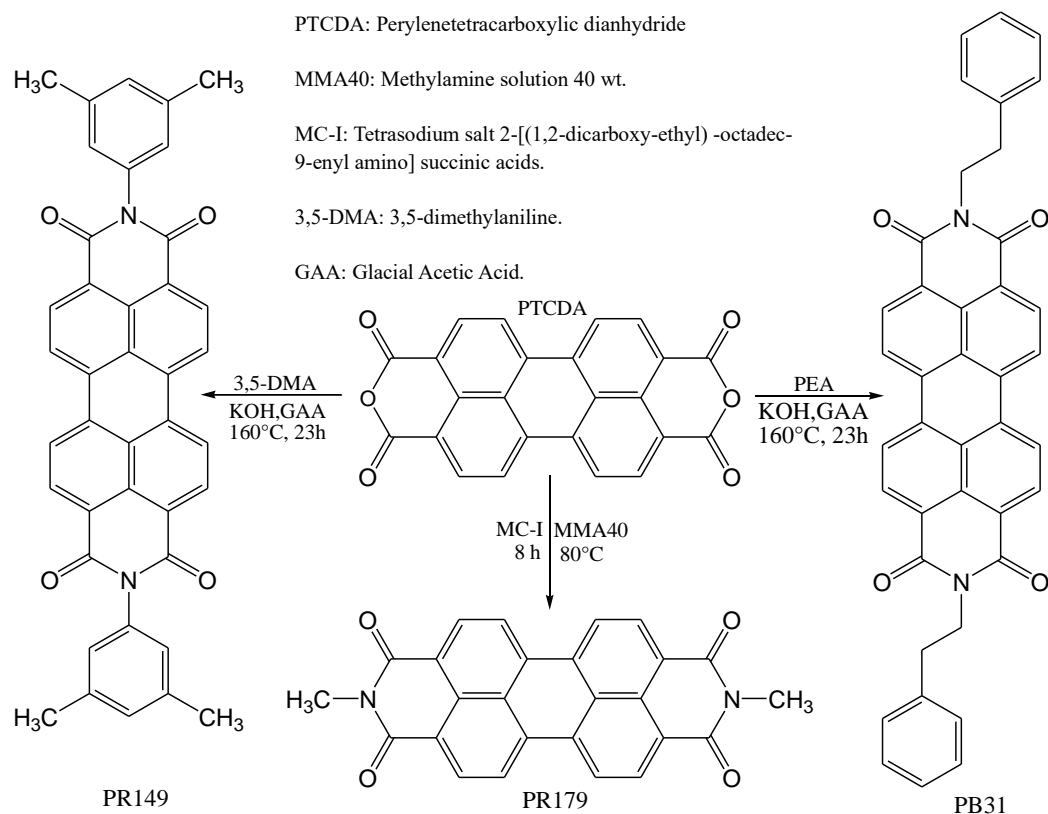


Figure 22. Synthesis of perylene pigments.

Table 4. Synthesis of PR 179: C₂₆H₁₄N₂O₄; M_w 418,4.

Name	CHN analysis (%)	Yield (%)	Colour
	Cal: C, 74.64; H, 3.37; N, 6.70		
FA-01-07	Found: C, 73.96; H, 3.27; N, 6.73	95	Red
FA-02-07	Found: C, 73.17; H, 3.34; N, 6.71	95	
FA-03-07	Found: C, 74.47; H, 3.36; N, 6.67	89.9	
FA-04-07	Found: C, 74.55; H, 3.15; N, 5.69	62.7	
FA-05-07	Found: C, 74.58; H, 3.22; N, 6.72	96.8	
FA-06-07	Found: C, 73.98; H, 3.09; N, 6.30	96.86	
FA-07-07	Found: C, 74.12; H, 3.10; N, 6.51	96.86	
FA-08-07	Found: C, 74.63; H, 3.29; N, 6.35	88.4	
FA-09-07	Found: C, 73.97; H, 3.37; N, 6.05	93.2	
FA-10-07	Found: C, 74.49; H, 3.40; N, 6.36	90.5	
FA-11-07	Found: C, 73.80; H, 3.32; N, 6.32	90.5	

Table 5. Synthesis of PR 149: C₄₀H₂₆N₂O₄, M_w 598,7.

Name	CHN analysis (%) Cal: C, 80.25; H, 4.38; N, 4.68	Yield (%)	Colour
FA-01-04	Found: C, 79.15; H, 4.16; N, 4.42	90.8	Red
FA-02-04	Found: C, 80.40; H, 4.33; N, 4.37	66.4	
FA-03-04	Found: C, 78.92; H, 4.27; N, 4.14	92.7	
FA-04-04	Found: C, 80.28; H, 4.52; N, 4.56	87.3	
FA-05-04	Found: C, 80.26; H, 4.25; N, 5.01	90.5	
FA-06-04	Found: C, 80.44; H, 4.29; N, 5.07	89.5	
FA-07-04	Found: C, 78.97; H, 4.24; N, 4.41	76.3	
FA-08-04	Found: C, 79.96; H, 4.32; N, 4.46	68.3	
FA-09-04	Found: C, 79.41; H, 4.37; N, 4.14	47.3	
FA-10-04	Found: C, 80.39; H, 4.40; N, 4.28	91.2	

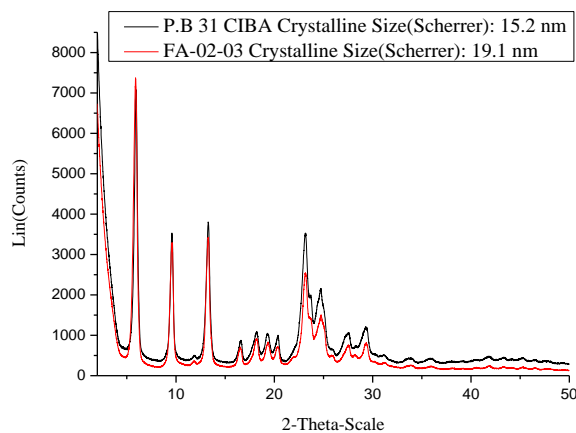
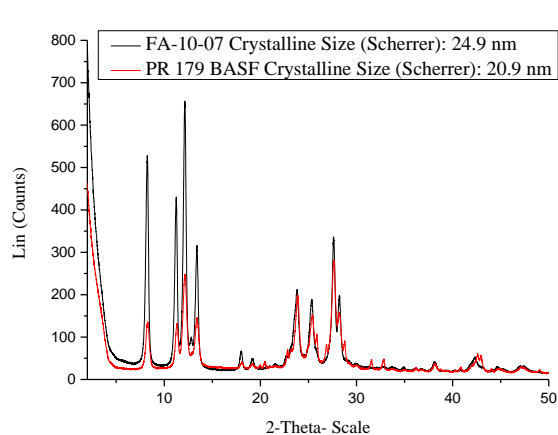
Table 6. Synthesis of Pigment Black 31: C₄₀H₂₆N₂O₄, M_w 598,7.

Name	CHN analysis (%) Cal: C, 80.25; H, 4.38; N, 4.68	yield	Colour
FA-01-03	Found: C, 80.76; H, 4.41; N, 4.53	90	Black
FA-02-03	Found: C, 80.62; H, 4.41; N, 4.62	95	

Table 7. Synthesis of cationic compounds.

Name	CHN analysis (%)	Yield (%)	Maldi	Colour
FA-DMPAPER	Cal: C, 72.84; H, 5.75; N, 9.99 Found: C, 73.08; H, 5.80; N, 9.66	85.3	OK	Red-brown
FA-BQPER 2	Cal: C, 50.13; H, 4.67; N, 6.50; I, 30.05 Found: C, 50.17; H, 4.54; N, 5.27; I, 32.5	90	OK	Red-Brown
FA-BQPER 3	Cal: C, 56.31; H, 5.22; N, 6.91; Br, 19.72 Found: C, 57.57; H, 5.31; N, 7.02; Br 18.31	93	OK	Red
FA-DMPANDI	Cal: C, 66.04; H, 6.47; N, 12.84 Found: C, 64.82; H, 6.30; N, 12.56	75	OK	Brown
FA-BQNDI 5	Cal: C, 43.35; H, 4.76; N, 7.78 Found: C, 42.16; H, 4.70; N, 7.51	96.7	OK	Yellowish-brown
FA-BQNDI 6	Cal: C, 48.99; H, 5.58; N, 8.16; Br, 23.28 Found C, 48.52; H, 5.27; N, 7.89; Br, 22.6	68.2	OK	Red
FA-BQPER7	Cal: C, 56.81, H, 6.16; N, 5.52; Br, 15.75 Found C, 57.52; H, 6.07; N, 5.85; Br, 6.39	75.4	OK	Brown-red

2.1.2. Powder X-ray diffraction:



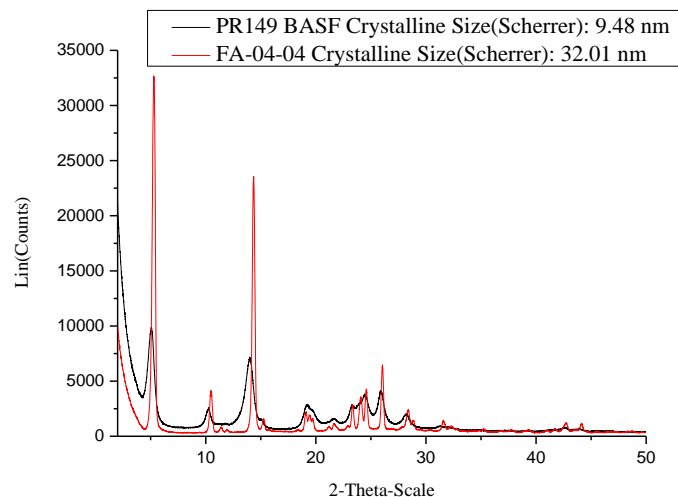


Figure 23. X-ray diffraction.

2.1.3. Spectral properties

The absorption and fluorescence spectra were measured on a Perkin-Elmer Lambda 35 UV / VIS Spectrophotometer in quartz cuvettes (1 cm). Concentrated sulfuric acid (96%) was used as a solvent. The absorption spectrum of the synthesis compounds from FA-01-07 to FA-13-07 shows absorption bands maxima at 552 nm and 595 nm which is identical to the absorption spectra of PR179 from BASF, and the absorption spectra of the synthesis compound from FA-01-04 to FA-10-04 shows absorption bands at 558 nm and 603 nm which is identical to the absorption spectra of PR179 from BASF, where the compounds FA-01-03 and FA-02-03 shows absorption bands maxima at 556 nm and 599 nm which is identical to the absorption spectra of PB31 from Ciba. From the luminescence measurement in concentrated sulfuric acid, one very important point is that the starting PTCDA beautifully redensities (fluoresces) red as well as red (tandem shifted) illuminates the condensation product with methylamine (PR 179) while the condensation product with 3,5-xylylidine (PR 149) is not luminescent, and the condensation product with PEA(PB31) show red fluoresces. All the synthesis products shows identical bands maxima with sample from company BASF and CIBA.

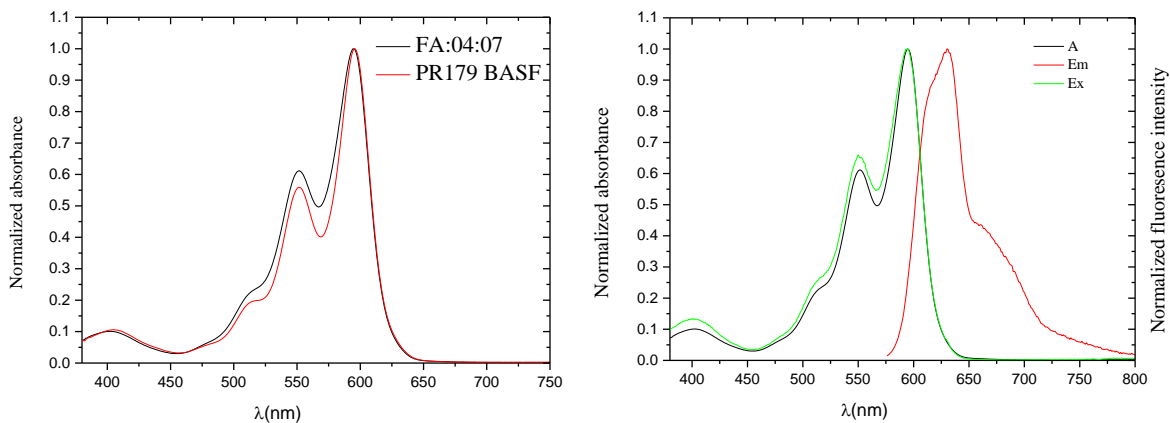


Figure 24. Left the absorption spectra of FA-04-07 shows identical peaks with BASF; Right. Absorption (A), Excitation (Ex), Fluorescence (Em) spectra of FA-04-07.

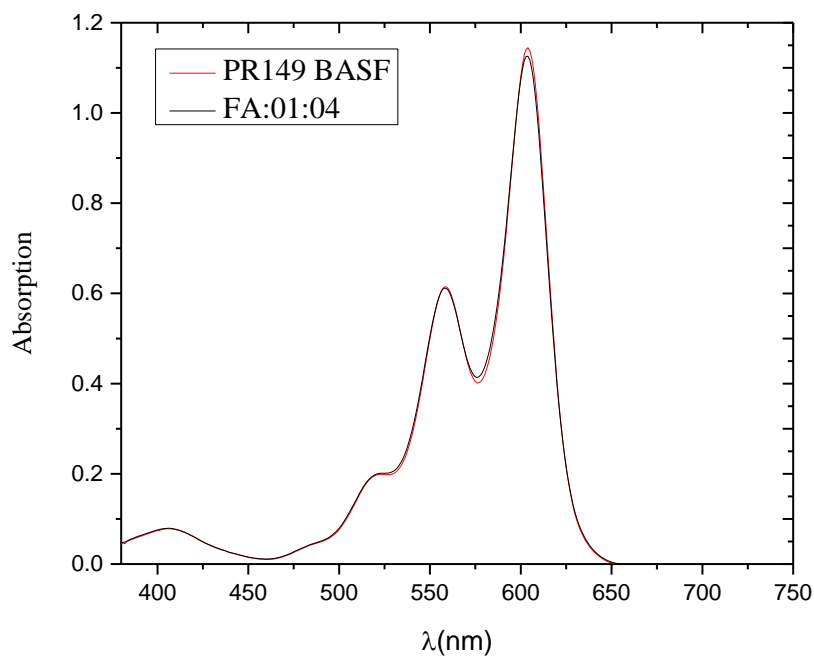


Figure 25. The absorption spectra of FA-01-04 shows identical peaks with PR 149 BASF.

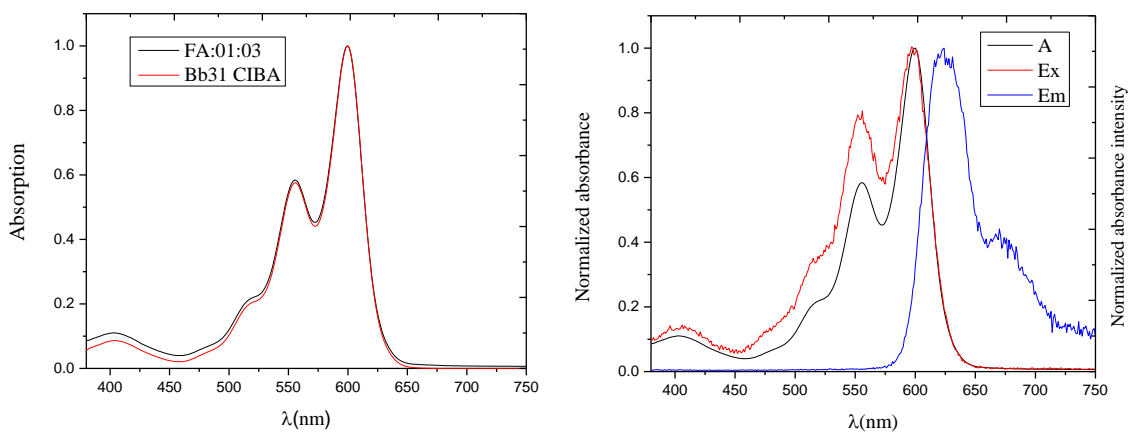


Figure 26. Left the absorption spectra of FA-01-03 shows identical peaks with CIBA; Right. Absorption (A), Excitation (Ex), Fluorescence (Em) spectra of FA-04-07.

2.1.4. EMS

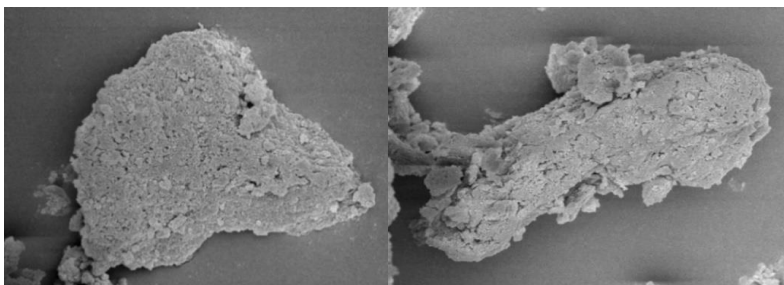


Figure 27. Left EMS of PR179 BASF, right EMS of FA-02-07 shows granular morphology emerges with size around 100 nm.

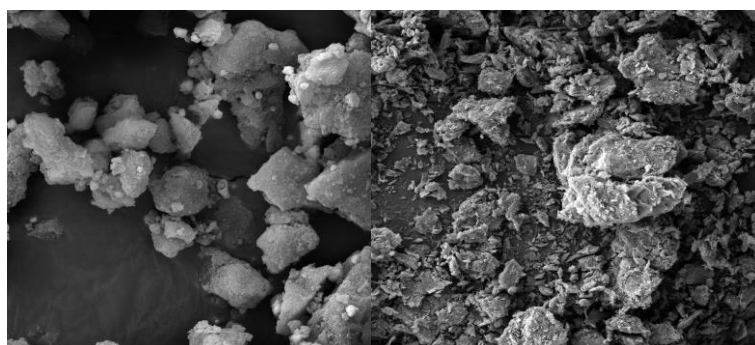


Figure 28. Left EMS of PR 179 BASF, right EMS of FA-07-07 shows a flower-like morphology with size around 100 nm.

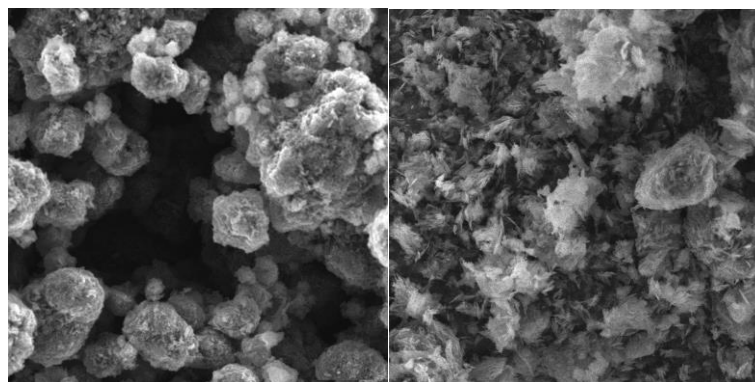


Figure 29. Left EMS of PB31 CIBA, right EMS of FA-01-03 shows a small crystal jointed together to form granules morphology with the size around 100 nm.

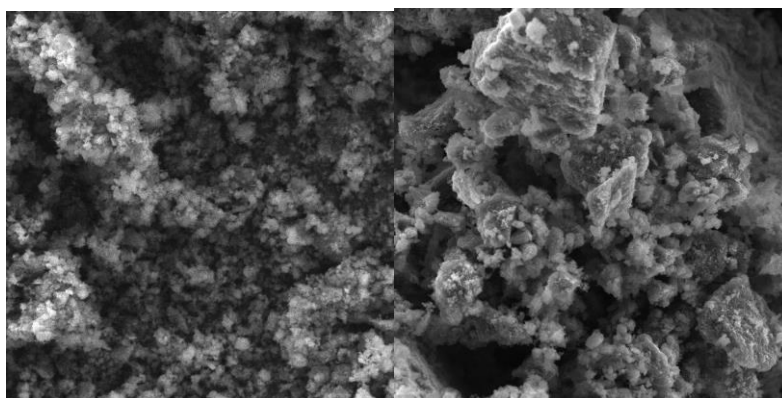


Figure 30. Left EMS of PR 149 BASF, right EMS of FA-01-04 shows crystal form granules morphology with the size around 100 nm.

2.1.5. Conclusion

Pigment Red 179 from foreign companies contains barium (Ba) in the form of BaSO_4 and organically bound barium. The proportion of both forms depends largely on who and in what quality the pigment is produced. As a note, here, that luminescence is an order of magnitude more sensitive than the UV / VIS absorption. So cleaning the crude pigments from luminescence more complex than just the removal of colored impurities. So, if we make a simple experiment, that the crude pigment PR 179, as it will filter out of the final reaction mixture, does not cleaned and "stir" in alkaline water (for better solubility applies KOH) and evaporated to give an intense yellow filtrate which luminescence strongly. Is a realistic assumption that this is probably a tetra salt, which strongly luminescence.

A single solvent PR 179 that has not yet found is concentrated sulphuric acid. The pigment is soluble because there is protonation of the molecule.

Table 8. The following table lists values of absorption peaks calculated where geometry optimization was performed by PM3 within the quantum-chemical program Zinda / S.

X	Y	λ_{max} (nm)
CH ₃ N	CH ₃ N	435
NH	CH ₃ N	435
NH	NH	434

O	CH ₃ N	433
O	NH	433
O	O	430

The calculations show that the individual molecules (in solution) are yellow with a small bathochromic shift from O to CH₃N. It is clear that the protonation of a molecule leads to a strong bathochromic shift. Moreover, the rigidity of the molecule leads to the protonated molecule in solution in sulfuric acid also strongly beautiful red luminescence (fluorescence).

Table 9. Absorption spectra of PTCDA and PR179.

Sample	λ_{\max} (nm)	A	ϵ_{\max} (dm ³ .g ⁻¹ .cm ⁻¹)	Ratio ϵ_1/ϵ_2
PTCDA	509	0.6049	151	1.6
	546	1	250	
PR179	595	0,751	188	1,77
	552	0,423	106	

Thus, absorption maxima are virtually identical (because the two maxima are vibronic structures) but differ in the size of the absorption coefficient. Pigment Red 149 can be made in a mixture of water and acetic acid, but because of the required reaction temperature (above 160 °C) this production requires an autoclave. The procedure in the autoclave leads to the desired product, which has a very nice blue shade and no luminescence.

3. Anti-corrosion and anti-microbial activity of perylene compounds and their application.

3.1. Anticorrosion inhibitor

Summary

Two pigment types (PDA-Mg, PDA-Zn) were synthesized, and their anticorrosion properties were evaluated and compared with those of an industrial corrosion inhibitor. The pigments were added to the epoxy-ester resin binder in concentrations of 0.10 wt.%, 0.25 wt.% and 0.50 wt.% and the paints so obtained were applied onto steel panels for testing. The reference paints contained the commercial Pigment Red 179 at 1 wt.% and the inert pigment TiO₂ to maintain a constant solid content of the paint. So, a blank and a reference system were obtained by using a paint with the commercial pigment and a paint with the industrial corrosion inhibitor, respectively. The solvent-based epoxy-ester resin was selected as the binder because it provides high-quality films suitable for corrosion protection of metallic substrates.

Keywords: perylene-3,4,9,10-tetracarboxylic acid salts; pigment; coating; corrosion; anticorrosion efficiency.

3.1.1. Results

3.1.2. Synthesis of perylene pigments

In the preparation of metal derivatives, proceed in two steps, i.e. preparation of a potassium salt (in water) and then reaction with a water-soluble divalent metal salt: general formula (Figure 31) as anti-corrosive pigments, wherein Me is Mg, Zn.

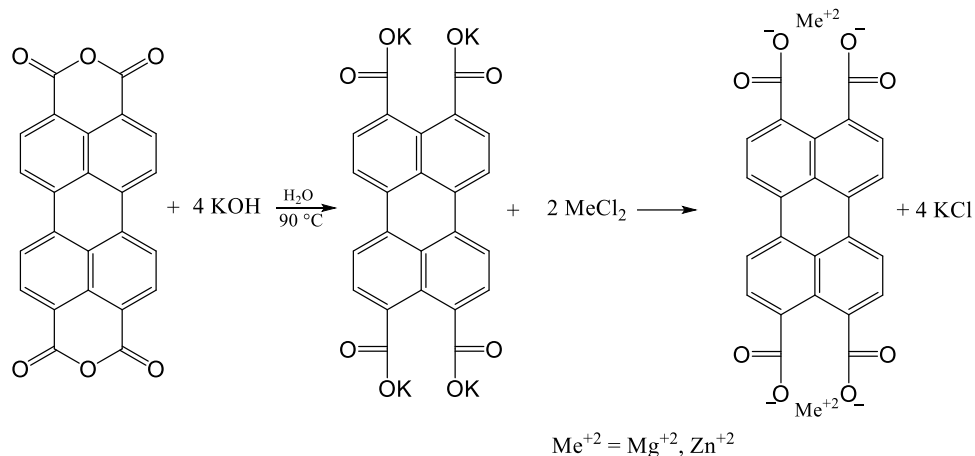


Figure 31. Structure scheme of perylene metal salt.

The yield of PDA-Mg was 5.44 g, representing 90.2 % based on the starting PTCDA. The Mg content of the PDA-Mg pigment was 101010 mg.kg⁻¹, in theory it should be 102800 mg.kg⁻¹.

The yield of PDA-Zn was 6.24 g, representing 82.8 % based on the starting PTCDA.

The Zn content of the PDA-Zn pigment was 213700 mg.kg⁻¹, in theory it should be 221200 mg.kg⁻¹.

Table 10. Neutral salt spray cyclic corrosion test:

Sample containing pigment	mass. %	Blisters		Delaminace in section /mm	Koroze	
		In the desktop /st.	in section /st.		in the desktop /%	in section /mm
P.R. 179	1	6MD	2D	21	0,3	5,3
PDA-Mg	0,1	8M	4M	16	0,3	1,9
	0,25	8M	4M	7	0,1	2,9
	0,50	8M	4MD	7	0,1	3,0
PDA-Zn	0,1	6MD	2MD	20	0,3	3,1
	0,25	6MD	2MD	23	0,3	4,3
	0,50	6MD	2M	14	0,3	3,2
Inhibitor	0,1	6M	2M	10	0,3	4,2
	0,5	6MD	2M	22	0,1	2,8
TiO₂	1,5	6MD	2D	17	3	7,3

Inhibitor = Ca salt of nitroisophthalic acid.

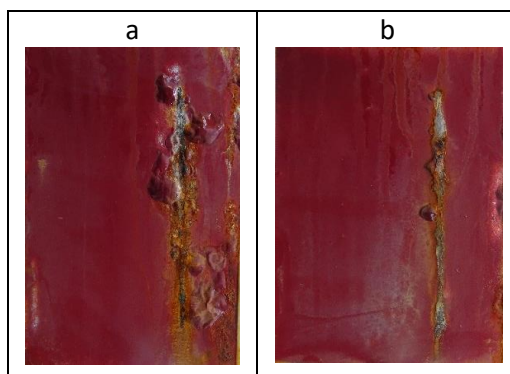


Figure 32. Images of selected organic coatings.

- a) an organic coating containing only Pigment Red 179,
 b) an organic coating comprising Pigment Red 179 and a PDA-Mg pigment (0.25 wt%).

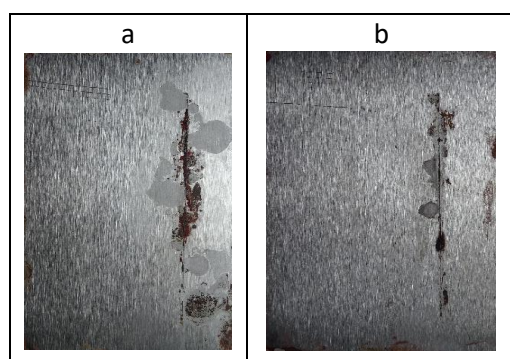


Figure 33. Steel panel images.

- a) an organic coating containing only Pigment Red 179,
 b) an organic coating comprising Pigment Red 179 and a PDA-Mg pigment (0.25 wt%).

Table 11. Results of electrochemical technique of linear polarization (DFT = $70 \pm 5 \mu\text{m}$).

Sample containing pigment	Mass. %	Before exposure		After 480 exposures in an atmosphere containing SO ₂	
		Polarization resistance/ Ω	Corrosion rate/mm year ⁻¹	Polarization resistance/ Ω	Corrosion rate /mm year ⁻¹
RED 179	1	$5,54 \times 10^6$	$14,8 \times 10^{-6}$	$9,65 \times 10^4$	$13,3 \times 10^{-4}$
PDA-Mg	0,1	$2,21 \times 10^8$	$36,9 \times 10^{-8}$	$1,22 \times 10^6$	$10,3 \times 10^{-6}$
	0,25	$6,86 \times 10^8$	$14,8 \times 10^{-8}$	$3,65 \times 10^7$	$17,8 \times 10^{-7}$
	0,50	$6,44 \times 10^8$	$14,1 \times 10^{-8}$	$2,95 \times 10^7$	$17,9 \times 10^{-7}$
PDA-Zn	0,1	$1,66 \times 10^8$	$28,5 \times 10^{-8}$	$2,02 \times 10^5$	$35,9 \times 10^{-5}$
	0,25	$3,75 \times 10^8$	$16,2 \times 10^{-8}$	$6,17 \times 10^6$	$11,6 \times 10^{-6}$
	0,50	$3,68 \times 10^8$	$16,8 \times 10^{-8}$	$2,21 \times 10^6$	$23,2 \times 10^{-6}$
Inhibitor	0,1	$5,44 \times 10^6$	$93,2 \times 10^{-7}$	$36,3 \times 10^6$	$11,6 \times 10^{-6}$
	0,5	$1,51 \times 10^7$	$76,4 \times 10^{-7}$	$1,34 \times 10^6$	$46,8 \times 10^{-6}$
TiO₂	1,5	$3,41 \times 10^5$	$29,5 \times 10^{-5}$	$41,2 \times 10^3$	$10,3 \times 10^{-3}$

Organic coatings containing synthesized PDA-Mg and PDA-Zn pigments achieved one order of magnitude lower corrosion rates. For these organic coatings (PDA-Mg), lower values of corrosion rate were achieved by coatings with a higher content of given pigments (corrosion rate $17,8 \times 10^{-7}$ mm / year at 0.25 wt.% and $17,9 \times 10^{-7}$ mm / year at 0,5 wt.%).

3.1.3. Conclusion

The objective of this work was to synthesize and describe the new perylene acid Mg^{2+} and Zn^{2+} salts, and also the perylene bis-imide derivatives of perylene, to study their anticorrosion capacity when the pigments used in epoxy ester resin-based coatings. The compounds PDA-Zn and PDA-Mg were successfully prepared and characterized by analytical methods (SEM, EDX, X-ray). The results of both the cyclic corrosion tests and electrochemical linear polarization measurements gave evidence of a high anticorrosion strength resistance of the perylene acid salts $\text{C}_{24}\text{H}_{12}\text{O}_{10}\text{Zn}_2$ and $\text{C}_{24}\text{H}_8\text{O}_8\text{Mg}_2$ at pigment volume concentrations of 0.25% and 0.5%. Their mechanism of action was mainly in their complexation capacity at the metal surface/organic coating/corrosive medium interface. The test results were compared with the simulated corrosion tests in the atmosphere containing NaCl or SO_2 with the electrochemical method of measurement by linear polarization. Moreover, coatings containing the pigment PDA-Mg showed a higher corrosion inhibitory effect, which was demonstrated by electrochemical tests compared to coatings containing PDA-Zn. The decrease in value in the corrosion rates (v_{corr}) of coatings containing the pigment PDA-Mg was lower after 480 h exposure in an atmosphere containing SO_2 (reduction in the corrosion rate by one to two orders of magnitude) than in the case of the coating containing the pigment PDA-Zn (reduction in the corrosion rate by two to three orders of magnitude) compared to the values of corrosion rates measured before the exposure of the samples in the above test. This conclusion was also confirmed by the evaluation of the measured polarization resistance (R_p). In the case of the pigment PDA-Mg, the protective mechanism was enhanced by the formation of a more chemically active basic $\text{Mg}(\text{OH})_2$. Mechanical tests gave evidence that the perylene-type pigments had no adverse effects on the systems mechanical properties: the mechanical resistance attained maximum levels.

Chapter 3

3.2. Anti-corrosion of azo carboxylate ligands.

Introduction

This work is concerning on a novel anti-corrosion magnesium complex for use in primer paints to protect the steel as anticorrosion inhibitors, corrosion products are formed at the metal-environment interface, by applying a thin layer of the inhibitor to the metal surface coating inhibitor or adsorption of the inhibitor formation of a thin film of particles.[12] The use of corrosion inhibitors is an effective solution to deal with corrosion, but we must realize that no

inhibitor is effective in all corrosive environments and for all metals, the effect of inhibitors is therefore specific (in protecting steel with organic substances).[13] Magnesium complexes with a new series of azo carboxylate ligands prepared from diazo-coupling reaction of anthranilic acid with 5-Methyl-2-phenyl-3-pyrazolone, anthranilic acid with naphthol AS-PH, anthranilic acid with 2-Naphthol and 2-Amino-5-nitrophenol with naphthol AS-PH were prepared. The metal complexes of azo compounds have been used as pigments, paints and other coloring materials.[14] the metal-azo complexes are one of the important molecules can make efficient thermal stability of organic dyes, therefore it has much attention in both academic and applied research [15–16]. This work study reporting four dyes and four metal complexes have been synthesized and characterized using elemental analysis, energy dispersive X-ray (EDX), matrix-assisted laser desorption/ ionization-time of flight (MALDI-TOF), X-ray Powder Diffraction (XRD).

3.2.1. Results

3.2.2. Synthesis of magnesium complex

In the synthesis of azo dyes and magnesium chloride where the ratio is 1:1 molar reaction ratio, the compounds were obtained in good yield, and they are soluble in most of the common organic solvents. the synthesis of azo-carboxylate ligand (figure 35) where the preparation by diazo-coupling reaction of anthranilic acid and 5-Methyl-2-phenyl-3-pyrazolone is described, for example, in the literature procedures [17, 18, 19]. The synthesized following a procedure that was slightly modified from that described in literature procedures for similar azo dyes.

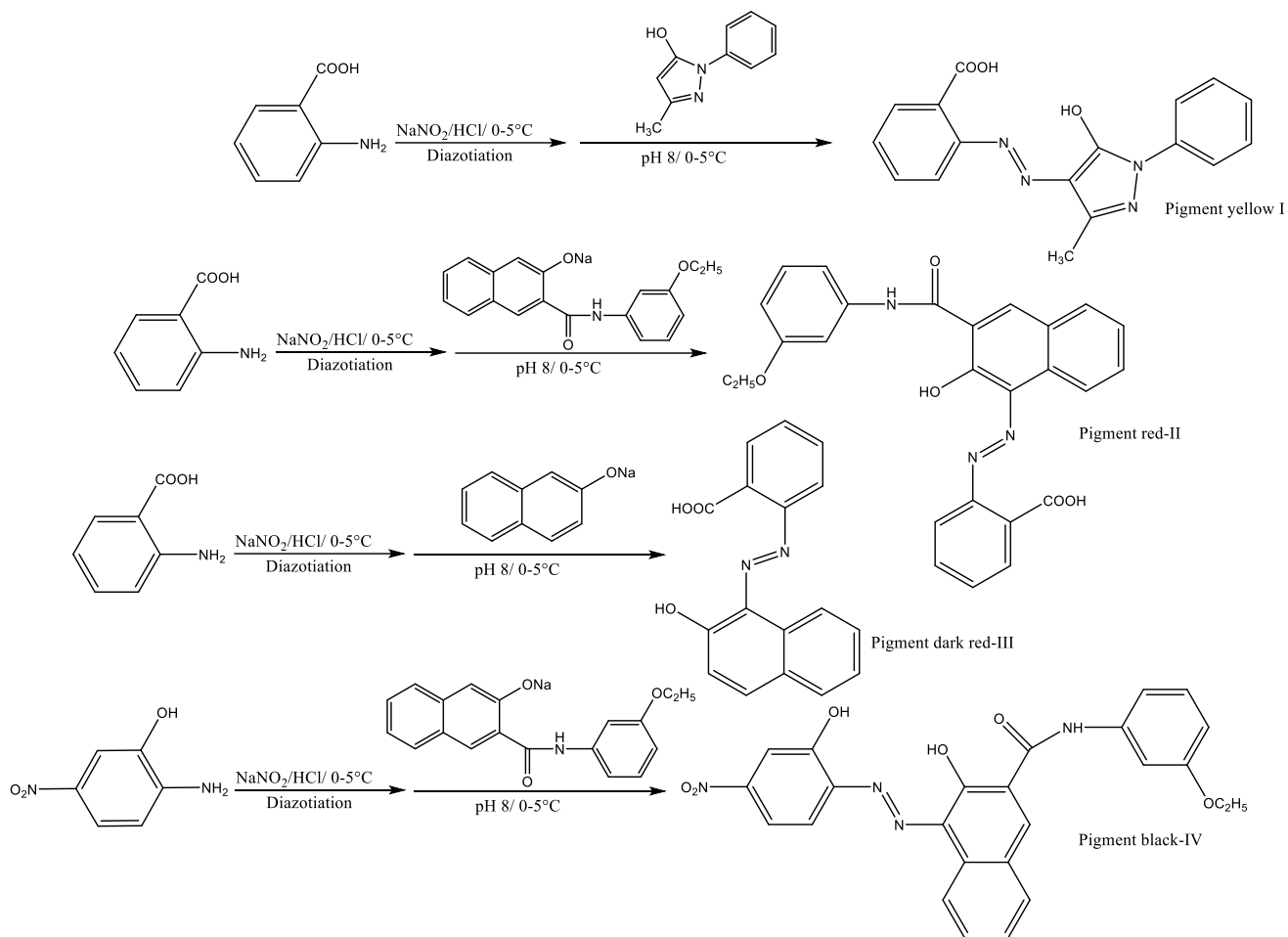


Figure 34. Chemical structure of Pigment Yellow-I, Pigment Red-II, Pigment Dark Red-III, and Pigment Black-IV.

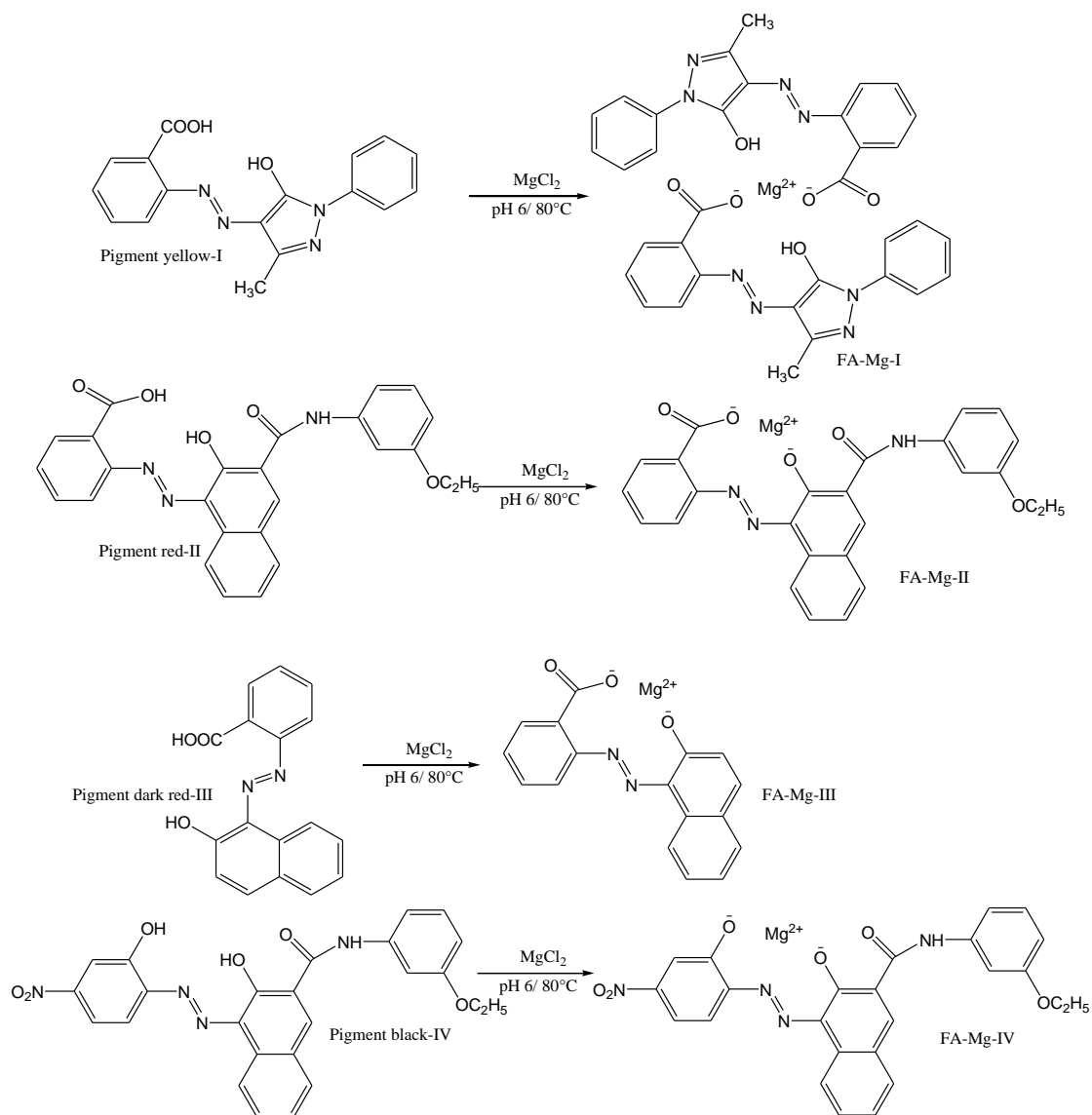


Figure 35. Synthesis of FA-Mg-I, FA-Mg-II, FA-Mg-III and FA-Mg-IV.

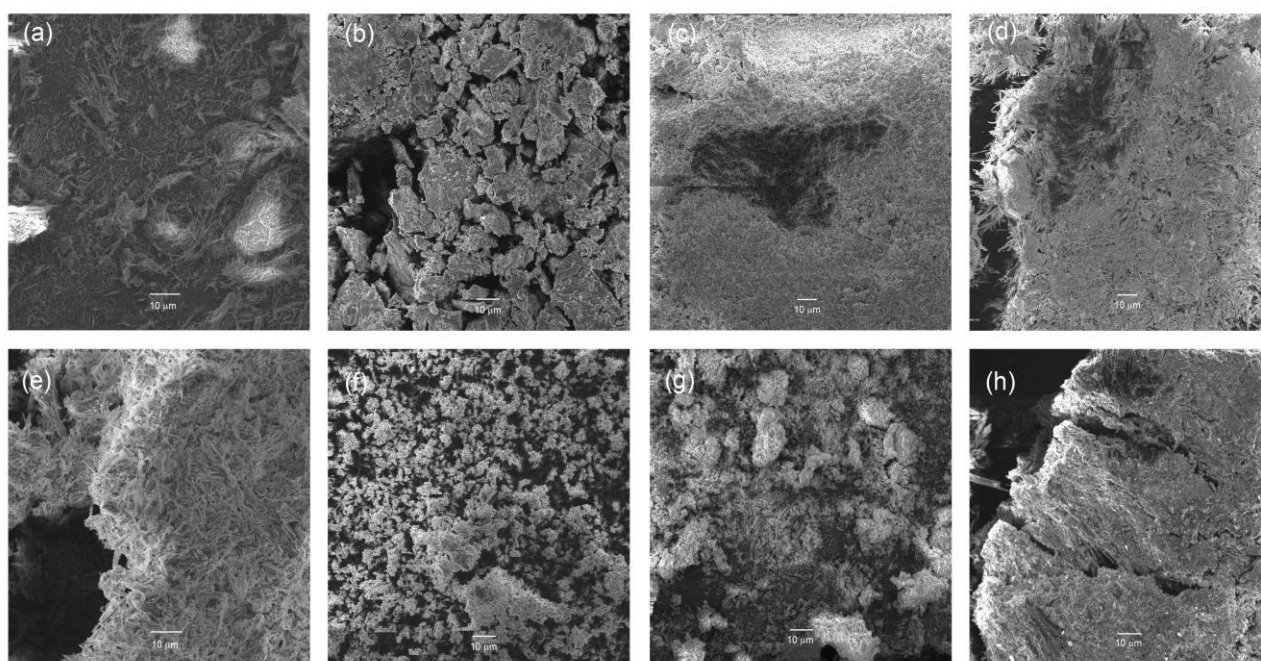
3.2.3. Physical properties of prepared pigments (Table 12) and magnesium complex (Table 13).

Table 12:

Pigments	Elemental analysis			Yield*(%)	Maldi
	C %	H %	N%		
Pigment yellow-I $\text{C}_{17}\text{H}_{14}\text{N}_4\text{O}_3$; $M_w = 322.32 \text{ g.mol}^{-1}$	Cal: 63.35 Found: 58.21	4.38 3.84	17.38 15.69	97.4	OK
Pigment red-II $\text{C}_{26}\text{H}_{21}\text{N}_3\text{O}_5$; $M_w = 455.47 \text{ g.mol}^{-1}$	Cal: 68.56 Found: 62.53	4.65 4.11	9.23 8.20		
Pigment dark red-III $\text{C}_{17}\text{H}_{12}\text{N}_2\text{O}_3$; $M_w = 292.29 \text{ g.mol}^{-1}$	Cal: 69.86 Found: 70.48	4.14 3.99	9.58 8.14	89.9	OK
Pigment black-IV $\text{C}_{25}\text{H}_{20}\text{N}_4\text{O}_6$; $M_w = 472.46 \text{ g.mol}^{-1}$	Cal: 63.56 Found: 60.92	4.27 4.39	11.86 11.08		

Table 13:

Pigments	Elemental analysis				Yield*(%)	Maldi
	C %	H %	N%	Mg%		
FA-Mg-I $C_{34}H_{26}MgN_8O_6$; $M_w = 666.9 \text{ g.mol}^{-1}$	Cal: 58.09 Found: 56.70	4.30 4.36	15.94 15.28	3.46 4.14	68.3	OK
FA-Mg-II $C_{26}H_{19}MgN_3O_5$; $M_w = 477.76 \text{ g.mol}^{-1}$	Cal: 65.36 Found: 62.61	4.01 4.63	8.80 8.17	5.59 5.09		
FA-Mg-III $C_{17}H_{10}MgN_2O_3$; $M_w = 314.58 \text{ g.mol}^{-1}$	Cal: 58.24 Found: 54.06	4.02 3.77	7.99 7.20	6.93 7.15	97.5	OK
FA-Mg-IV $C_{25}H_{18}MgN_4O_6$; $M_w = 494.75 \text{ g.mol}^{-1}$	Cal: 56.57 Found: 53.67	4.18 4.12	10.56 9.67	4.58 4.32		

3.2.4. SEM: Scanning electron microscope.**Figure 36.** Scanning electron microscope.

It can be seen from (Figure 36) the SEM image of Pigment Yellow-I(a) shows homogeneity in the form of strings crystal, Pigment Red-II (b) shows leaching appears to etch the surface morphology emerges, Pigment Dark Red-III (c) shows granular morphology emerges, Pigment Black-IV (d) shows crystal form of needles. All compounds from (a) to (d) show a morphology with a crystal size of around 100 nm. The SEM images of the magnesium complexes: FA-Mg-I (e) shows homogeneity in the form of sharp superficial flakes, FA-Mg-II (f) shows homogeneity in the form of an aggregate of thin superficial plates, FA-Mg-III (g) shows homogeneity in the form of granular morphology, FA-Mg-IV (h) shows homogeneity in the form pure crystal surface morphology. All magnesium complexes from (e) to (h) show clean morphology with crystal size around 100 nm.

3.2.5. X-ray powder diffraction

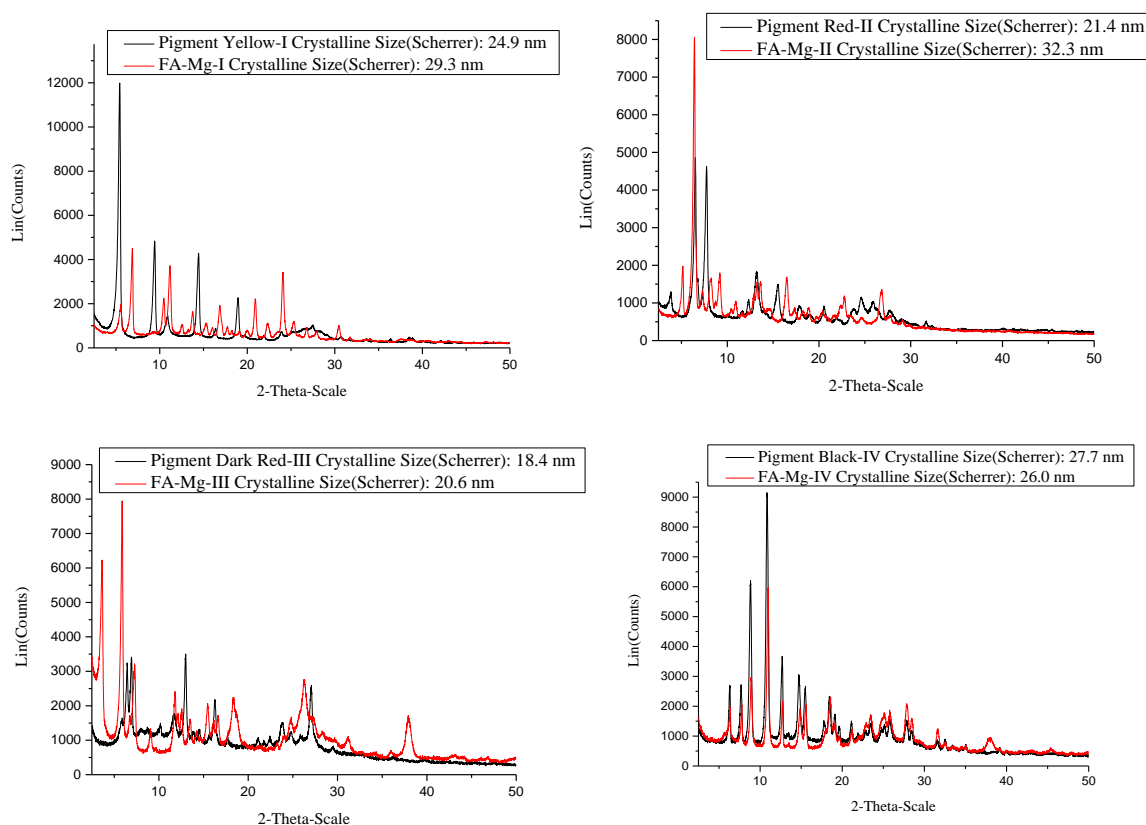


Figure 37. X-ray powder diffraction.

3.2.1. Spectral properties

The absorption and fluorescence spectra were measured on a Perkin-Elmer Lambda 35 UV / VIS Spectrophotometer in quartz cuvettes (1 cm). Acetone was used as a solvent.

Table 14. The absorption values and the absorption coefficient for the pigments and magnesium complexes in acetone.

Sample	λ max (nm)	A	ϵ_{max} ($\text{dm}^3 \cdot \text{g}^{-1} \cdot \text{cm}^{-1}$)
Pigment Yellow-I	387	0.44904	62
Pigment Red-II	488	0.34128	43
	511	0.33609	43
Pigment Dark Red-III	469	0.38176	52
Pigment Black-IV	511	0.49518	62
	537	0.4568	57
FA-Mg-I	387	0.18807	27
FA-Mg-II	494	0.25919	37
	513	0.25205	36
FA-Mg-III	470	0.79725	11
	491	0.75710	11
FA-Mg-IV	515	0.35560	48
	540	0.36809	50

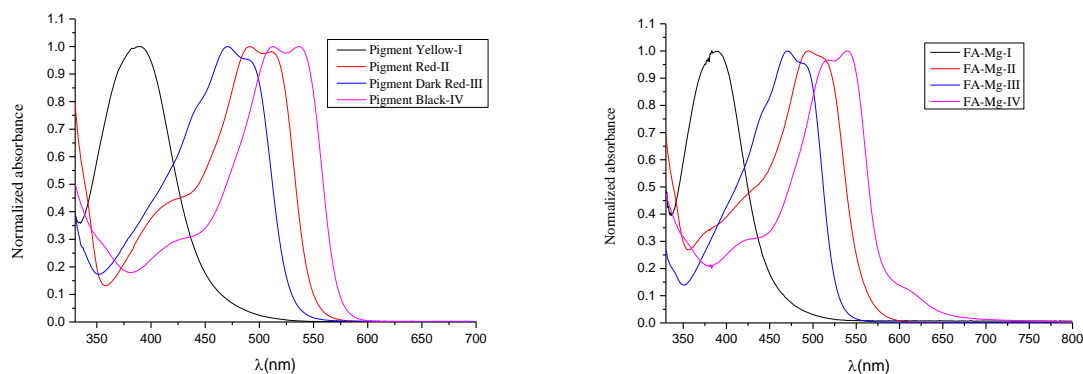


Figure 38. UV–vis Spectra of the compounds in acetone.

Azo dyes contain intramolecular charge-transfer chromophores and therefore, their UV–vis absorption bands depend on the combination of electron-donating and withdrawing moieties in the molecules. The peak absorption values and the absorption coefficient for the pigments and magnesium complexes in acetone are reported in Table 13. The absorption band of Pigment Yellow-I, Pigment Red-II, Pigment Dark Red-III, Pigment Black-IV appears about 387; 488, 511; 469; 511, 537 nm, respectively, and the absorption band of the FA-Mg-I, FA-Mg-II, FA-Mg-III and FA-Mg-IV appears about 387; 494, 513; 470, 491; 515, 540 nm respectively. The absorption spectra of these pigments show a prominent band between 387 and 537 nm assigned to the π – π^* transitions. Where the magnesium complexes show a prominent band between 387 and 540 nm.

3.2.2. Pigment specification:

The four-magnesium complexes were subjected to measurements of the typical paint parameters, i.e. density and oil number, which served to calculate the critical pigment volume concentration (CPVC) of each complex. The results are listed in Table 23. The densities of magnesium complexes lay within the range from 1.37 to 1.55 $\text{g}\cdot\text{cm}^{-3}$; the oil numbers lay between 43.2 and 75.8 g / 100 g of the complex; and the CPVC values were 46–59. Zinc nitroisophthalate density was 2.60 $\text{g}\cdot\text{cm}^{-3}$, oil number 42 g / 100 g of the pigment; and CPVC was 43. For TiO_2 the respective values were 4.12 $\text{g}\cdot\text{cm}^{-3}$, 27 g / 100 g of the pigment, and 45.

Table 15. Characteristics of the fabricated complexes: density, oil number and critical pigment volume concentration (CPVC).

Complex	Density [g/cm^3]	Oil absorption [g/100g]	CPVC [-]
FA-Mg-I $\text{C}_{34}\text{H}_{26}\text{MgN}_8\text{O}_6$	1.38±0.02	45.9	59
FA-Mg-II	1.37 ± 0.02	56.8	54

$C_{26}H_{19}MgN_3O_5$			
FA-Mg-III	1.55 ± 0.02	43.2	58
$C_{17}H_{10}MgN_2O_3$			
FA-Mg-IV	1.41 ± 0.02	75.8	46
$C_{25}H_{18}MgN_4O_6$			

Table 16. Results of the corrosion test performed in a condenser chamber filled with the atmosphere containing SO_2 of the studied organic coatings after 1536 hours of exposure, DFT = $90 \pm 10 \mu m$:

Pigment	PVC [%]	Blistering		Corrosion	
		Metal base [dg]	In the cut [dg]	In the cut [mm]	Metal base [%]
FA-Mg-I $C_{34}H_{26}MgN_8O_6$	1	8F	4D	3- 3.5	3
	3	6M	2D	3- 3.5	0.03
	5	6F	2D	3- 3.5	1
	10	8F	4MD	2- 2.5	0.1
FA-Mg-II $C_{26}H_{19}MgN_3O_5$	1	8MD	8F	0.5- 1	-
	3	8M	6M	0.5- 1	0.03
	5	8D	2MD	0- 0.5	-
	10	8MD	8F	0- 0.5	-
FA-Mg-III $C_{17}H_{10}MgN_2O_3$	1	8MD	4MD	0- 0.5	1
	3	-	8F	0- 0.5	50
	5	8M	4F	0- 0.5	3
	10	6M	6M	0.5- 1	10
FA-Mg-IV $C_{25}H_{18}MgN_4O_6$	1	6F	8F	0.5- 1	3
	3	6M	-	1-1.5	0.03
	5	6M	-	0- 0.5	3
	10	8D	8D	0- 0.5	0.03

Table 17. Results of the electronic linear polarization measurements for organic coatings pigmented with organic pigments and with Zn content at Q = 60%. DFT = $50 \pm 5 \mu m$:

Sample containing pigment	PVC [%]	Electrochemical linear polarization	
		Polarization resistance/ Ω	Corrosion rate/mm year ⁻¹
FA-Mg-I $C_{34}H_{26}MgN_8O_6$	1	2.31×10^{10}	4.40×10^{-9}
	3	2.32×10^{10}	4.42×10^{-9}
	5	2.49×10^{10}	4.40×10^{-9}
	10	2.50×10^{10}	4.11×10^{-9}
FA-Mg-II $C_{26}H_{19}MgN_3O_5$	1	1.19×10^{10}	8.42×10^{-9}
	3	1.15×10^{10}	8.49×10^{-9}
	5	1.14×10^{10}	8.70×10^{-9}

	10	1.17×10^{10}	8.85×10^{-9}
FA-Mg-III $C_{17}H_{10}MgN_2O_3$	1	1.32×10^{10}	7.33×10^{-9}
	3	1.34×10^{10}	7.24×10^{-9}
	5	1.98×10^{10}	5.07×10^{-9}
	10	2.20×10^{10}	4.65×10^{-9}
FA-Mg-IV $C_{25}H_{18}MgN_4O_6$	1	7.84×10^9	1.11×10^{-8}
	3	7.83×10^9	1.09×10^{-8}
	5	7.68×10^9	1.08×10^{-8}
	10	8.17×10^9	1.05×10^{-8}

3.2.4. Conclusion

The pigments were characterized (determination of oil number and density) to calculate the value of CPVC (critical volume concentration of pigment) which was necessary for the assembly formulation of paint materials. The pigments with Mg have oil numbers in a range of values 43.2 – 75.8. The highest value of 75.8 g/100 g of pigment was found for the FA-Mg-IV ($C_{25}H_{18}MgN_4O_6$). The complex FA-Mg-IV has a relatively large particle porosity and therefore a large surface area can be assumed capable of adsorption. The densities of the new Mg-containing organic pigments were measured in the range of 1.37–1.55 g·cm⁻³. The measured values of linseed oil consumption and density, it was then calculated CPVC value. CPVC values increased with decreasing oil numbers in the range of 46–59. The highest CPVC value was achieved by FA-Mg-I. The steel panels with an organic coating of DFT = 90 ± 10 μm corrosion changes due to the influence of the neutral salt fog environment. Corrosive action was evaluated every 7 days (168 hours) and ended after 1680 hours. The amount of blisters in the area and in the section and corrosion in the area and in the section were evaluated (Table 26–27). The organic coatings with a content of magnesium, coatings with FA-Mg-I achieved the highest anti-corrosion efficiency. These the coatings at all PVC values showed no corrosion of the coating and blistering in the area were found after 1680 hours only at the PVC value = 1 % (6F). At the same time, all coatings showed the lowest rate of corrosion at the point of the test cut (1.5–3.5 mm). Blisters in the section at values of PVC = 1 and 3 %, they reached a rating of 6M and at values of PVC = 5 and 10 %, they reached a rating of 4M. Organic coatings with FA-Mg-I at PVC values = 3, 5 and 10 % extra reached only a very small degree of under-

corrosion of the steel panel, which decreased with increasing the PVC value (in the range of 0.03 - 0.1 %).

Chapter 4

4. Anti-Microbial activity of Perylene Compounds.

Introduction

The antimicrobial activity effect of the compounds tested on *Staphylococcus aureus*, *Escherichia coli*, and *Candida albicans*. The work was done to contribute and understanding the self-assembly of perylene bisimide dyes in water and help to develop applications of those systems. The substituents are necessary to act as solubility enhancing of the perylene core. The polarity and ability of water to act as hydrogen bond donors and acceptors results in weakened electrostatic and dipole interactions. The aim of this work is to prepare perylene bisimide dyes which are soluble in water through bisimide chromophores by the introduction of the N,N-Dimethyl-1,3-propanediamine via the imide position, which become water-soluble upon protonation by different types of spacers. The second part of the work is to use these cationic compounds by dyeing with cellulose and testing the biological activity of the compounds. Antibiotics have crucial importance to increase their resistance to bacteria, several researches are trying to discover and develop methods for antimicrobial effectiveness. In this study, the antimicrobial activities of synthesized perylene diimides compounds were tested, perylene diimides well known as pigments and dyes for various applications and also antimicrobial activities. These compounds were determined against strain *Staphylococcus aureus*, *Escherichia coli*, and *Candida albicans*. The antimicrobial activity of the compounds with polypropylene shows an effect on *Staphylococcus aureus*, *Escherichia coli*, and *Candida albicans*, and the compounds dyeing with cellulose show a reduction in the growth of *Staphylococcus aureus*.

4.1. Results

4.1.2. Synthesis of cationic compounds.

The cationic compounds were synthesized by the following literature procedures with minor modification [20]. Where the DMPA-PER and DMPA-NDI were synthesized by UPa procedure. The cationic FA-BQPER and FA-BQNDI contain two positive charges and thus show considerable water solubility.

$C_{34}H_{32}N_4O_4$; $M_w = 560.65 \text{ g.mol}^{-1}$	Found: 73.08	5.80	9.66	-	85.3	-
FA-BQPER 2	Cal: 51.20	4.54	6.63	30.05		
$C_{36}H_{38}N_4O_4I_2$; $M_w = 844.53 \text{ g.mol}^{-1}$	Found: 50.17	4.54	5.27	32.5	90	OK
FA-DMPA-NDI	Cal: 66.04	6.47	12.84	-		
$C_{24}H_{28}N_4O_4$; $M_w = 436.51 \text{ g.mol}^{-1}$	Found: 64.82	6.30	12.56	-	75	-
FA-BQNDI 5	Cal: 43.35	4.76	7.78	35.23		
$C_{26}H_{34}N_4O_4I_2$; $M_w = 720.39 \text{ g.mol}^{-1}$	Found: 42.16	4.70	7.51	21.7	96.7	OK

Table 19:

Compounds	Elemental analysis				Yield*(%)	Maldi
	C %	H %	N%	Br%		
FA-BQPER 3	Cal: 56.31	5.22	6.91	19.72		
$C_{38}H_{42}N_4O_6Br_2$; $M_w = 810.58 \text{ g.mol}^{-1}$	Found: 57.57	5.31	7.02	18.31	93	OK
FA-BQNDI 6	Cal: 48.99	5.58	8.16	23.28		
$C_{28}H_{38}N_4O_6Br_2$; $M_w = 686.44 \text{ g.mol}^{-1}$	Found: 48.52	5.27	7.89	22.6	68.2	OK
FA-BQPER 7	Cal: 56.81	6.16	5.52	15.75		
$C_{48}H_{62}N_4O_{10}Br_2$; $M_w = 1014.85 \text{ g.mol}^{-1}$	Found: 57.52	6.07	5.85	16.39	75.4	OK

4.1.3. SEM: Scanning electron microscope.

The SEM shows a nice crystal, which means that the compounds are clean. The compounds show homogeneity of the compounds without impurities, and the compounds DMPA-PDI, FA-BQPER 2 and FA-BQPER 3 show nice long rod crystal shapes in size around 100 nm.

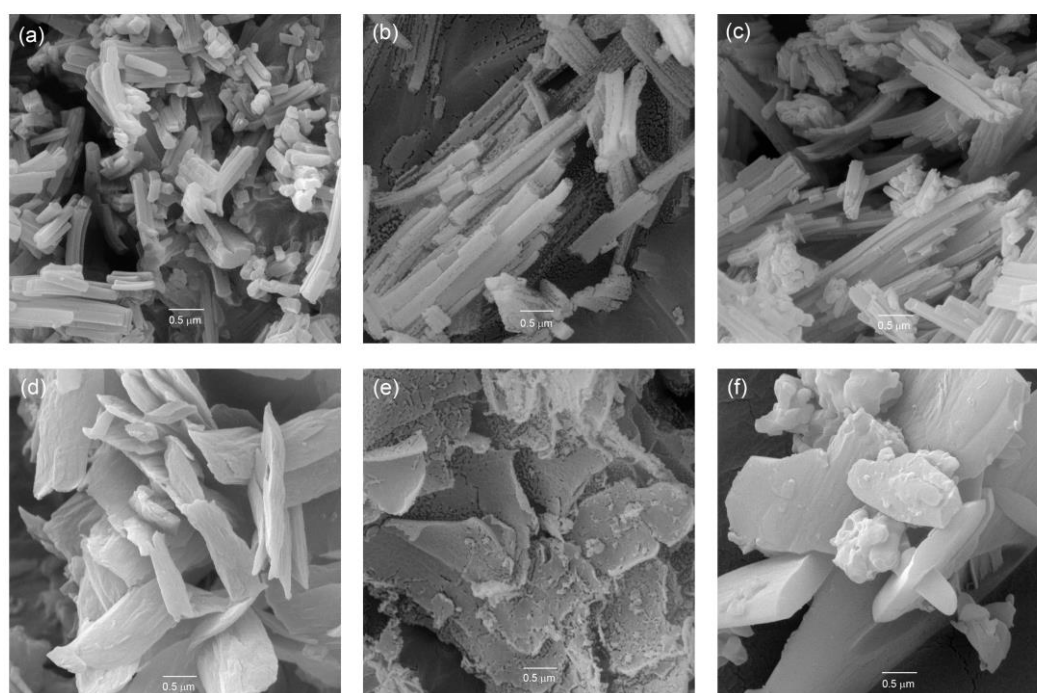


Figure 40. SEM results of the compounds (a) DMPA-PER; (b)FA-BQPER 2; (c) FABQPER 3; (d) DMPANDI; (e) FA-BQNDI 5; (f) FA-BQNDI 6.

4.1.4. Antimicrobial activity

Table 20. Results of antimicrobial activity of PP samples:

Name		<i>Staphylococcus aureus</i>			<i>Escherichia coli</i>			<i>Candida albicans</i>		
		N (CFU/cm ²)	log N	R	N (CFU/cm ²)	log N	R	N (CFU/cm ²)	log N	R
PP (reference)	Shaken immediately	8,2.10 ³	3,9	-	4,4.10 ⁴	4,7	-	1,0.10 ³	3,0	-
	with exposure	4,5.10 ⁴	4,7	-	6,0.10 ⁵	5,8	-	5,3.10 ⁴	4,7	-
	in the dark	9,3.10 ⁴	4,9	-	7,3.10 ⁵	5,9	-	6,4.10 ⁴	4,8	-
PP + BQPER 2	with exposure	1,6.10 ⁴	4,2	0,8	3,0.10 ⁵	5,5	0,3	9,2.10 ³	4,0	0,7
	in the dark	9,4.10 ⁴	4,9	0	3,1.10 ⁵	5,5	0,4	7,2.10 ³	3,9	0,9
PP + BQPER 3	with exposure	4,1.10 ³	3,6	1,4	2,7.10 ⁵	5,4	0,4	9,5.10 ¹	2,0	2,7
	in the dark	1,4.10 ⁴	4,2	0,8	3,7.10 ⁵	5,7	0,2	1,5.10 ³	3,2	1,6
PP+ 0,1 % BQNDI 2	with exposure	8,3.10 ⁵	5,92	0,13	1,2.10 ⁶	6,09	0,20	4,6.10 ⁴	4,66	0,11
	in the dark	7,6.10 ⁵	5,88	0,25	1,8.10 ⁶	6,26	0,04	8,0.10 ⁴	4,90	0,01
PP+ 0,1 % BQNDI 3	with exposure	5,9.10 ⁵	5,77	0,28	<1	-	≥6,29	2,0.10 ⁴	4,29	0,38
	in the dark	3,2.10 ⁵	5,50	0,63	1,4.10 ⁵	5,14	1,16	7,2.10 ⁴	4,86	0,05

Table 21. Results of the concentration of viable bacteria (c) and their logarithm:

Sample		<i>S. aureus</i> CCM 4516	
		c (CFU/ml)	log c
1 - 100% cotton MILETA, reference	Shaken immediately	1,2.10 ⁴	4,1
	Incubated with exposure	1,5.10 ³	3,2
	Incubated in the dark	1,5.10 ⁵	5,2
2 – 100% cotton + FA-BQPER 2, st. coloring 3 %, wt. XENOTEST 1, 3 %.	Shaken immediately	8,9.10 ²	2,9
	Incubated with exposure	< 1	0
	Incubated in the dark	3,0.10 ⁰	0,5
3 - 100% cotton + FA-BQPER 2, st. coloring 5 %, wt. XENOTEST 2, 5 %.	Shaken immediately	2,2.10 ³	3,3
	Incubated with exposure	< 1	0
	Incubated in the dark	1,0.10 ⁰	0
4 - 100% cotton + FA-BQPER 3, st. coloring 3 %, wt. XENOTEST 3, 3 %.	Shaken immediately	2,2.10 ³	3,3
	Incubated with exposure	< 1	0
	Incubated in the dark	2,5.10 ⁰	0,3
5 - 100% cotton + FA-BQPER 3, st. coloring 5 %, wt. XENOTEST 4, 5 %.	Shaken immediately	2,7.10 ⁴	4,4
	Incubated with exposure	< 1	0
	Incubated in the dark	< 1	0

Table 22. Interpretation of the results of the effectiveness of antibacterial properties.

Efficacy of antibacterial properties	Antibacterial effect value A
Weak	1 < A < 2
Significant*	2 ≤ A < 3
Strong *	A ≥ 3

* Values and efficiency have taken from ČSN EN ISO 20743: 2013.

4.1.5. Application and the affinity to Cotton

Color fastness to washing at 60 °C according to ČSN EN ISO 105 - C06 (800 120)



Figure 41. Dyed material: 100 % cotton with FA-BQPER 2.

Table 23:

Color shade 1% - color change	Staining cotton	Staining wool
4 – 5 R	3 – 4 Y	3 R
Color shade 2.5% - color change	Staining cotton	Staining wool
4 – 5 R	3 R	3 R
Color shade 5% - color change	Staining cotton	Staining wool
4 – 5 R	3 – 4 R	3 R

Wash fastness at 40°C and 60° C- ČSN EN ISO 105 – C06 (800 120).

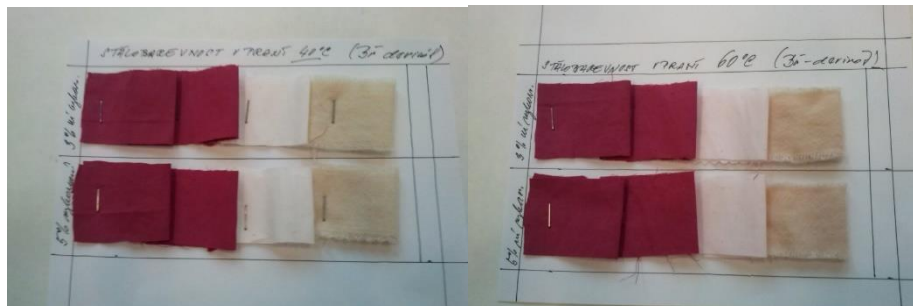


Figure 42. Dyed material: 100 % cotton with FA-BQPER 3

Table 24:

Wash fastness 40°C	Staining cotton	Staining wool
Color shade 3 % - color change 4 – 5 R	4	4
Color shade 5 % - color change 4 – 5 R	4	3 - 4

Table 25:

Wash fastness 60°C	Staining cotton	Staining wool
Color shade 3 % - colorchange 4 – 5 R	3	2 - 3
Color shade 5 % - color change 4 – 5 R	3	2

Table 26. LIGHTFASTNESS – XENOTEST (ISO 105-B02)

Sample	Lightfastness XENOTEST
FA-BQPER 2 Color shade 3%	3
FA-BQPER 2 Color shade 5%	3
FA-BQPER 3 Color shade 3%	3
FA-BQPER 3 Color shade 5%	3

Dyed material: 100% cotton. Evaluated immediately after the xenotest.



Figure 43. Compound BQPER 2 and BQPER 3.

If the samples are stored in the dark after the xenotest, the coloration will return to this level in a few days.

4.1.6. Conclusion

The cationic perylenes produce high slight amounts of singlet oxygen. The results show an indication of the effect of cationic perylenes at exposure. BQPER 2 at exposure shows a weak antibacterial effect against *S. aureus* and *Candida albicans*, the value of $R = 0.8$ in the dark against *S. aureus*, and the value of $R = 0.9$ against *Candida albicans* indicates a reduction in growth caused probably by the presence of iodine. BQPER 3 shows a weak antibacterial effect against *S. aureus*, and Significant antibacterial effect against *Candida albicans*. BQNDI 2 shows a weak antibacterial effect against *S. aureus*, *Escherichia coli* and *Candida albicans*. BQNDI 3 determined strong antibacterial activity at exposure against *Escherichia coli*, and weak antibacterial activity at dark. The value of $R < 0.5$ cannot be considered antibacterial, because for microbiological methods the usual error of determination is 0.5 log order.

The photoactive effect against the gram-positive bacterial strain *Escherichia coli* has so far been confirmed in a sample of PP film containing 0.1% by weight. BQNDI 3, which determined strong antibacterial activity at exposure and weak antibacterial activity without access to light.

References

- [1]. Law, Kock-Yee a Ihor W. Tarnawskyj. Azo pigments and their intermediates. A new class of couplers for red and near-IR sensitive photogenerating azo pigments. *Dyes and Pigments* [online]. 1994, 25(4), 281-293 [cit. 2022-08-04]. ISSN 01437208. Available from: doi:10.1016/0143-7208(94)87015-2.
- [2]. Udo Herrmann, Lothar Weismantel, Frank Linke, Ronald Gobel, Bernhard Krumbach, Wolfgang Frank, Appl.No: 09/821,888. Publ.No.:US 2001/0047087 A1, Nov.29,2001.
- [3] Manfred. Lorenz, Karl Heinz, Schündehütte Wolfgang. Bornatsch. Methods for the preparation of azo compounds, and azo compounds. Appl.No.: 83103747.8. Publ.No: EP0073463A1.09/1983.
- [4.] Gheorghiu C. et al, Rom. Revistade Chimie (1980), 31 (7), 632-7. ISSN: 0034-7752.
- [5]. Allan, J. R., Pendrowski, M. J., Gerrard, D. L., & Bowley, H. J. (1987). The thermal, spectral and magnetic studies of chloro and bromo compounds of cobalt (II), nickel (II) and copper (II) with melamine. *Thermochimica acta*, 115, 21-30.
- [6]. Manfred. Lorenz, Karl Heinz, Schündehütte Wolfgang. Bornatsch. Methods for the preparation of azo compounds, and azo compounds. Appl.No.: 83103747.8.Publ.No: EP0073463A1.09/1983.
- [7].(a) Linke Frank. Faubion Kent. Herrmann Udo. Pfützenreuter Dirk. Göbel Ronald. Metal complex pigments, Appl.No 99119099.2. Publ.No: EP 0 994 162 A1. (b)Herrmann Udo. Pfützenreuter Dirk. Göbel, Ronald. Metal complex pigments, Appl.No 99119099.2. Publ.No:

EP 0 994 162 B1.

- [8]. Ulrich Feldhues, Bergisch Gladbach, Frank Linke, Ronald Gobel, appl.No.:11/824,787, Int.Cl.G03F 1/00(2006.01), Pub.No.: US 2008/0057417 A1, Pub.Date: Mar.6,2008.
- [9]. Shimada Katsunori. Shoji Fumiko. Organometallic complex, method for producing the same and pigment. Appl.No.:JP 2004-89040, Cl.C09B045-14, Pub.No.: JP 2005272688 A, Oct 6, 2005.
- [10]. Mizuguchi, J., and K. Tojo. 2002. "Electronic Structure of Perylene Pigments as Viewed from the Crystal Structure and Excitonic Interactions". *The Journal of Physical Chemistry B* 106 (4): 767-772. <https://doi.org/10.1021/jp012909p>.
- [11]. Kobitski, A.Yu, R Scholz, and D.R.T Zahn. 2003. "Theoretical studies of the vibrational properties of the 3,4,9,10,-perylene tetracarboxylic dianhydride (PTCDA) molecule". *Journal of Molecular Structure: THEOCHEM* 625 (1-3): 39-46. [https://doi.org/10.1016/S0166-1280\(02\)00755-8](https://doi.org/10.1016/S0166-1280(02)00755-8).
- [12] G., Camila a Alexandre F. Corrosion Inhibitors – Principles, Mechanisms and Applications. In: ALIOFKHAZRAEI, M., ed. *Developments in Corrosion Protection* [online]. InTech, 2014, 2014-02-20 [cit. 2022-08-12]. ISBN 978-953-51-1223-5. doi:10.5772/57255.
- [13] NOVÁK, Pavel. *Koroze kovů*. Praha: Ústav kovových materiálů a korozního inženýrství, Fakulta chemické technologie Vysoká škola chemicko-technologická v Praze .
- [14] MANKU, G.S., R.C. CHADHA, N.K. NAYAR a M.S. SETHI. The formation constants of lanthanon(III) complexes with some 1-(substituted)phenylazo-2-naphthols. *Journal of the Less Common Metals* [online]. 1971, 25(1), 55-59 [cit. 2022-08-12]. ISSN 00225088. doi:10.1016/0022-5088(71)90065-8.
- [15] SEYBOLD, G. *Farbenchemie: Color Chemistry. Synthesis, Properties and Applications of Organic Dyes and Pigments*. Von H. Zollinger, VCH Verlagsgesellschaft, Weinheim 1987. 367 S., geb. 198,- DM. ISBN 3-527-26200-8. *Nachrichten aus Chemie, Technik und Laboratorium* [online]. 1987, 35(12), 1264-1265 [cit. 2022-08-12]. ISSN 03415163. doi:10.1002/nadc.19870351215.
- [16] FRANKEL, Max. *Azo and Diazo Chemistry, Aliphatic and Aromatic Compounds*, by Heinrich Zollinger, Interscience Publishers Inc, New York, 1961, pp. 444. Price \$ 16.50. *Israel Journal of Chemistry* [online]. 1963, 1(1), 45-45 [cit. 2022-08-12]. ISSN 00212148. doi:10.1002/ijch.196300014.
- [17] ROY, Manojit, Sanasam Sachika DEVI, Subhadip ROY, C.B. SINGH a Keisham Surjit SINGH. Synthesis, characterization, crystal structures and in vitro antimicrobial activities of triorganotin(IV) complexes of azo-dicarboxylates. *Inorganica Chimica Acta* [online]. 2015, 426, 89-98 [cit. 2022-08-12]. ISSN 00201693. doi: 10.1016/j.ica.2014.11.030.
- [18] Lyčka, A, D Luštinec, J Holeček, M Nádvorník a M Holčapek. 27Al, 15N, 13C and 1H NMR spectra and negative-ion electrospray mass spectra of the 2: 1 aluminium (III) complexes of azo dyes derived from anthranilic acid. *Dyes and Pigments* [online]. 2001, 50(3), 203-209 [cit. 2022-08-12]. ISSN 01437208. doi:10.1016/S0143-7208(01)00049-3.
- [19] Smitha, P., S. K. Asha a C. K. S. Pillai. Synthesis, characterization, and hyperpolarizability measurements of main-chain azobenzene molecules. *Journal of Polymer Science Part A: Polymer Chemistry* [online]. 2005, 43(19), 4455-4468 [cit. 2022-08-12]. ISSN 0887-624X. doi:10.1002/pola.20922.

[20] Ji, Wei, Xue Zhang, Jianzhang Zhao, Ye Gao, Wei Song a Yukihiro Ozaki. In situ formation of SERS hot spots by a bis-quaternized perylene dye: a simple strategy for highly sensitive detection of heparin over a wide concentration range. *The Analyst* [online]. 2018, 143(8), 1899-1905 [cit. 2022-12-09]. ISSN 0003-2654. doi:10.1039/C8AN00015H

List of documents related to the dissertation work

Patents and utility models

Hrdina R., Steinfeld J., Burgert L., Gotzman R., Chaloupka J., Florián Č., Vlk M., Beneš L., Fouzy A., Vyňuchal J.: Method for producing a yellow pigment based on a complex of nickel cation, melamine and azobarbituric acid and a new crystal modification of this pigment that can be prepared in this way. CZ 304515 B6 20140611.

Output (commercialization): production of Pigment Yellow 150 under the trade name Versal Yellow 9GP at Synthesia a.s.

Hrdina R., Burgert L., Kalendová A., Alafid F., Panák O., Držková M., Kohl M.: Use of perylenic acid salts as anticorrosive substances. CZ 308991 B6 20200416.

Držková M., Panák O., Hrdina R., Alafid F., Vyňuchal J., Gotzmann R., Lišková V., Valtr J.: Thermochromic paint, Utility model: CZ 35 445 U1. 2021.

A1 - publications in foreign and international peer reviewed journals (journals with impact factor)

Maixner J., Rohlíček J., Florián Č., Vyňuchal J., Alafid F.: X-ray powder diffraction data for monosodium salt azobarbituric acid dihydrate. *Powder Diffraction* 29 (4), December (2014), 383-384. doi: <https://doi.org/10.1017/S0885715614000657>. (Year 2021: Impact Factor of Journal 2.544, Journal Rank Q2).

Kohl M., Alafid F., Bouška M., Krejčová A., Raycha Y., Kalendová A., Hrdina R., Burgert L.: New Corrosion Inhibitors Based on Perylene Unit in Epoxy Ester Resin Coatings. *Coatings* 2022, 12, 923. <https://doi.org/10.3390/coatings12070923>. (Year 2021: Impact Factor of Journal 3.236, Journal rank Q2.).

B1 - Lectures at foreign conferences or at important international conferences held in the Czech Republic

Alafid F., Hrdina R., Burgert L.: Preparation and Properties of Perylene Dyes. 7th International Conference on Chemical Technology, 15-17 April, Mikulov, 2019. (Lecture). PÁLAVA HALL-PT8. ISBN 978-80-88307-00-6.

B2 - Foreign conference posters or at important international conferences held in the Czech Republic

Hrdina R., Alafid F., Přichystal P., Vyňuchal J.: The preparation of colorants in MW reactors and some technological aspects. XXII Encontro nacional da SPQ, 3.–6. July 2011, Braga, Portugal. Poster QO CP 94.

Alafid F., Hrdina R.: New Metal Complex Pigments Based on Azobarbituric acid". BOSS/XIII, 13th Belgian Organic Synthesis Symposium, Leuven, Belgium, July 15. 20, 2012 (Poster P013). ISSN 0213-3911.

Alafid F., Hrdina R., Černý M., Burgert L.: Preparation of High Performance Perylene Colorants, ICCT 2018, 16. – 18. April 2018, Mikulov. Czech Republic. Poster P51, ISBN 978-80-86238-77-7.

C1 - Domestic conference lectures

Alafid F., Hrdina R., Burgert L., Bouška M., Pummerová M., Pištěková H., Sedlařík V., Kubáč L., Trousil V., Vyňuchal J., Valtr J., Němec M., Procházková B., Lovecká P.: Cationic perylene dyes. XIV. Konference pigmenty a pojiva, 15.-16. listopad 2021, Kongresový hotel Jezerka v Seči u Chrudimi. Abstract: ISBN 978-80-906269-6-6.

Kohl M., Alafid F., Kalendová A., Hrdina R.: Formulation of anti-corrosion coating moths with synergistic action of metallic zinc and pigments containing magnesium. XIV. Konference pigmenty a pojiva, 15.-16. listopad 2021, Kongresový hotel Jezerka v Seči u Chrudimi. Full text: ISBN 978-80-906269-6-6.

Kubáč L., Černý J., Bečvaříková R., Hrdina R., Burgert L., Alafid F., Pummerová M., Pištěková H., Sedlařík V., Lišková V.: Photoactive perylene derivatives as additives for polymer matrix with self-cleaning properties. XIV. Konference pigmenty a pojiva, 15.-16. listopad 2021, Kongresový hotel Jezerka v Seči u Chrudimi. Abstract: ISBN 978-80-906269-6-6.

Hrdina R., Burgert L., Kalendová A., Alafid F., Bayerová P., Čermý M., Brožková I., Moťková P., Krejčová A., Pummerová M., Pištěková H., Sedlařík V., Kubáč L., Trousil V., Vyňuchal J., Valtr J., Němec M., Procházková B., Lovecká P.: Antimicrobial fiber treatments – Dichtung und Wahrheit. XIV. Konference pigmenty a pojiva, 15.-16. listopad 2021, Kongresový hotel Jezerka v Seči u Chrudimi. Abstract: ISBN 978-80-906269-6-6.

Hrdina R., Kohl M., Kalendová A., Alafid F., Burgert L.: Corrosion inhibition capabilities of perylene pigments in organic coatings based on epoxy ester resin. XII. konference pigmenty a pojiva, 11.-12. listopad 2019, Kongresový hotel Jezerka v Seči u Chrudimi. Abstract: ISBN 978-80-906269-4-2.

Kalendová A., Hrdina R., Kohl M., Alafid F., Burgert L.: Corrosion inhibition capabilities of perylene pigments in organic coatings based on epoxy ester resin. XII. konference pigmenty a pojiva, 11.-12. Listopad 2019, Kongresový hotel Jezerka v Seči u Chrudimi. ISBN 978-80-906269-4-2.

Alafid F., Hrdina R.: Preparation of HP pigments in a microwave reactor. APROCHEM 2011, 11. – 13.4.2011, Jeseníky, Hotel Dlouhé stráně. ISBN 978-80-02-02306-7, full text p. 220-229.

Alafid F., Hrdina R., Burgert L.: Preparation of Pigment Yellow 138. APROCHEM 2010, 21. –23.4.2010, Jeseníky, Hotel Dlouhé stráně. ISBN 978-80-02-02212-1, full text p. 1258-1266.

C2 - Domestic conference posters

Držková M., Panák O., Vyňuchal J., Gotzmann R., Lišková V., Valtr J., Alafid F., Hrdina R.: Cationic perylene dyes. XIV. Konference pigmenty a pojiva, 15.-16. listopad 2021, Kongresový hotel Jezerka v Seči u Chrudimi. Abstract: ISBN 978-80-906269-6-6.